



DOEET147004

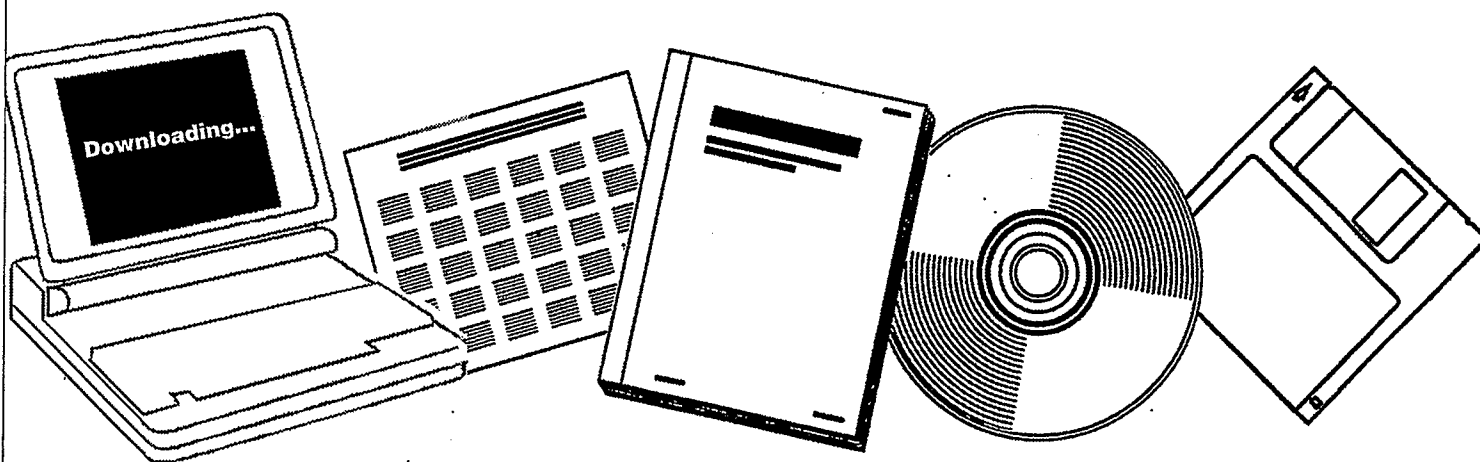
**NTIS**

One Source. One Search. One Solution.

**CHEMISTRY AND CATALYSIS OF COAL  
LIQUEFACTION CATALYTIC AND THERMAL  
UPGRADING OF COAL LIQUID AND HYDROGENATION  
OF CO TO PRODUCE FUELS. QUARTERLY PROGRESS  
REPORT, JULY-SEPTEMBER 1980**

UTAH UNIV., SALT LAKE CITY. DEPT. OF  
MINING AND FUELS ENGINEERING

FEB 1981



U.S. Department of Commerce  
**National Technical Information Service**

DOEET147004



DOE/ET/14700-4

Distribution Category UC-90d

Chemistry and Catalysis of Coal Liquefaction  
Catalytic and Thermal Upgrading of Coal Liquid  
and Hydrogenation of CO to Produce Fuels

Quarterly Progress Report  
for the Period July - Sept 1980

Dr. Wendell H. Wiser

University of Utah - Department of  
Mining and Fuels Engineering  
Salt Lake City, Utah 84112

Date Published - February, 1981

Prepared for the United States Department  
of Energy  
Under Contract No. DE-AC01-79ET14700

## CONTENTS

I	Cover Sheet	1
II	Objective and Scope of Work	3
III	Highlights to Date	7
IV	Task 1 Chemical-Catalytic Studies	Inactive
	Task 2 Carbon-13 NMR Investigation of CDL and Coal	8
	Task 3 Catalysis and Mechanism of Coal Liquefaction	21
	Task 4 Momentum, Heat and Mass Transfer in Co-Current Flow	25
	Task 5 The Fundamental Chemistry and Mechanism of Pyrolysis of Bituminous Coal	32
	Task 6 Catalytic Hydrogenation of CD Liquids and Related Polycyclic Aromatic Hydrocarbons	33
	Task 7 Denitrogenation and Deoxygenation of CD Liquids and Related N- and O- Compounds	35
	Task 8 Catalytic Cracking of Hydrogenated CD Liquids and Related Hydrogenated Compounds	38
	Task 9 Hydropyrolysis (Thermal Hydrocracking) of CD Liquids	Inactive
	Task 10 Systematic Structural-Activity Study of Supported Sulfide Catalysts for Coal Liquids Upgrading	53
	Task 11 Basic Study of the Effects of Coke and Poisons on the Activity of Upgrading Catalysts	Inactive
	Task 12 Diffusion of Polyaromatic Compounds in Amorphous Catalyst Supports	57
	Task 13 Catalyst Research and Development	60
	Task 14 Characterization of Catalysts and Mechanistic Studies	64
V	Conclusion	68

## II OBJECTIVE AND SCOPE OF WORK

### I. The chemistry and Catalysis of Coal Liquefaction

#### Task 1 Chemical-Catalytic Studies

Coal will be reacted at subsoftening temperatures with selective reagents to break bridging linkages between clusters with minimal effect on residual organic clusters. The coal will be pretreated to increase surface area and then reacted at 25 to 350°C. Reagents and catalysts will be used which are selective so that the coal clusters are solubilized with as little further reaction as possible.

#### Task 2 Carbon-13 NMR Investigation of CDL and Coal

Carbon-13 NMR spectroscopy will be used to examine coal, coal derived liquids (CDL) and residues which have undergone subsoftening reactions in Task 1 and extraction. Improvements in NMR techniques, such as crosspolarization and magic angle spinning, will be applied. Model compounds will be included which are representative of structural units thought to be present in coal. Comparisons of spectra from native coals, CDL and residues will provide evidence for bondings which are broken by mild conditions.

#### Task 3 Catalysis and Mechanism of Coal Liquefaction

This fundamental study will gain an understanding of metal salt chemistry and catalysis in coal liquefaction through study of reactions known in organic chemistry. Zinc chloride and other catalytic materials will be tested as Friedel-Crafts catalysts and as redox catalysts using coals and selected model compounds. Zinc chloride, a weak Friedel-Crafts catalyst, will be used at conditions common to coal liquefaction to participate in well defined hydrogen transfer reactions. These experiments will be augmented by mechanistic studies of coal hydrogenation using high pressure thermogravimetric analysis and structural analysis. The results of these studies will be used to develop concepts of catalysis involved in coal liquefaction.

#### Task 4 Momentum Heat and Mass Transfer in CoCurrent Flow of Particle-Gas Systems for Coal Hydrogenation

A continuation of ongoing studies of heat and transport phenomena in cocurrent, co-gravity flow is planned for a one-year period. As time and development of existing work permits, the extension of this study to include a coiled reactor model will be undertaken. Mathematical models of coal hydrogenation systems will utilize correlations from these straight and coiled reactor configurations.

#### Task 5 The Fundamental Chemistry and Mechanism of Pyrolysis of Bituminous Coal

Previous work at the University of Utah indicates that coal pyrolysis, dissolution (in H-donor) and catalytic hydrogenation all have similar rates and activation energies. A few model compounds will be pyrolyzed in the range of 375 to 475°C. Activation energies, entropies and pro-

duct distributions will be determined. The reactions will assist in formulating the thermal reaction routes which also can occur during hydro-liquefaction.

## II. Catalytic and Thermal Upgrading of Coal Liquids

### Task 6 Catalytic Hydrogenation of CD Liquids and Related Polycyclic Aromatic Hydrocarbons

A variety of coal derived (CD) liquids will be hydrogenated with sulfided catalysts prepared in Task 10 from large pore, commercially available supports. The hydrogenation of these liquids will be systematically investigated as a function of catalyst structure and operating conditions. The effect of extent of hydrogenation will be the subject of study in subsequent tasks in which crackability and hydrolysis of the hydrogenated product will be determined. To provide an understanding of the chemistry involved, model polycyclic arenes will be utilized in hydrogenation studies. These studies and related model studies in Task 7 will be utilized to elucidate relationships between organic reactants and the structural-topographic characteristics of hydrogenation catalysts used in this work.

### Task 7 Denitrogenation and Deoxygenation of CD Liquids and Related Nitrogen- and Oxygen-Containing Compounds

Removal of nitrogen and oxygen heteroatoms from CD liquids is an important upgrading step which must be accomplished to obtain fuels corresponding to those from petroleum sources. Using CD liquids as described in Task 6, exhaustive HDN and HDO will be sought through study of catalyst systems and operating conditions. As in Task 6, catalysts will be prepared in Task 10 and specificity for N- and O-removal will be optimized for the catalyst systems investigated. Model compounds will also be systematically hydrogenated using effective HDN/HDO catalysts. Kinetics and reaction pathways will be determined. A nonreductive denitrogenation system will be investigated using materials which undergo reversible nitridation. Conditions will be sought to cause minimal hydrogen consumption and little reaction of other reducible groups.

### Task 8 Catalytic Cracking of Hydrogenated CD Liquids and Related Polycyclic Naphthenes and Naphthenoaromatics

Catalytic cracking of hydrogenated CD liquid feedstocks will be studied to evaluate this scheme as a means of upgrading CD liquids. Cracking kinetics and product distribution as a function of preceding hydrogenation will be evaluated to define upgrading combinations which require the minimal level of CD liquid aromatic saturation to achieve substantial heteroatom removal and high yields of cracked liquid products. Cracking catalysts to be considered for use in this task shall include conventional zeolite-containing catalysts and large-pore molecular sieve, CLS (cross-linked smectites) types under study at the University of Utah. Model compounds will be subjected to tests to develop a mechanistic understanding of the reactions of hydro CD liquids under catalytic cracking conditions.

### Task 9 Hydropyrolysis (Thermal Hydrocracking) of CD Liquids

Heavy petroleum fractions can be thermally hydrocracked over a specific range of conditions to produce light liquid products without excessive hydrogenation occurring. This noncatalytic method will be applied to a variety of CD liquids and model compounds, as mentioned in Task 6, to determine the conditions necessary and the reactivity of these CD feedstocks with and without prior hydrogenation and to derive mechanism and reaction pathway information needed to gain an understanding of the hydropyrolysis reactions. Kinetics, coking tendencies and product compositions will be studied as a function of operating conditions.

### Task 10 Systematic Structural-Activity Study of Supported Sulfide Catalysts for Coal Liquids Upgrading

This task will undertake catalyst preparation, characterization and measurement of activity and selectivity. The work proposed is a fundamental study of the relationship between the surface-structural properties of supported sulfide catalysts and their catalytic activities for various reactions desired. Catalysts will be prepared from commercially available. Supports composed of alumina, silica-alumina, silica-magnesia and silica-titania, modification of these supports to change acidity and to promote interaction with active catalytic components is planned. The active constituents will be selected from those which are effective in a sulfided state, including but not restricted to Mo, W, Ni and Co. The catalysts will be pre-sulfided before testing. Catalyst characterization will consist of physico-chemical property measurements and surface property measurements. Activity and selectivity tests will also be conducted using model compounds singly and in combination.

### Task 11 Basic Study of the Effects of Coke and Poisons on the Activity of Upgrading Catalysts

This task will begin in the second year of the contract after suitable catalysts have been identified from Tasks 6, 7 and/or 10. Two commercial catalysts or one commercial catalyst and one catalyst prepared in Task 10 will be selected for a two-part study, (1) simulated laboratory poisoning/coking and (2) testing of realistically aged catalysts. Kinetics of hydrogenation, hydrodesulfurization, hydrodenitrogenation and hydrocracking will be determined before and after one or more stages of simulated coking. Selected model compounds will be used to measure detailed kinetics of the above reactions and to determine quantitatively how kinetic parameters change with the extent and type of poisoning/coking simulated. Realistically aged catalysts will be obtained from coal liquids upgrading experiments from other tasks in this program or from other laboratories conducting long-term upgrading studies. Deactivation will be assessed based on specific kinetics determined and selective poisoning studies will be made to determine characteristics of active sites remaining.

### Task 12 Diffusion of Polyaromatic Compounds in Amorphous Catalyst Supports

If diffusion of a reactant species to the active sites of the catalyst is slow in comparison to the intrinsic rate of the surface reaction, then only sites near the exterior of the catalyst particles will be utilized effectively. A systematic study of the effect of molecular size on the sorptive diffusion kinetics relative to pore geometry will

be made using specific, large diameter aromatic molecules. Diffusion studies with narrow boiling range fractions of representative coal liquid will also be included. Experimental parameters for diffusion kinetic runs shall include aromatic diffusion model compounds, solvent effects, catalyst sorption properties, temperature and pressure.

### III. Hydrogenation of CO to Produce Fuels

#### Task 13 Catalyst Research and Development

Studies with iron catalysts will concentrate on promoters, the use of supports and the effects of carburizing and nitriding. Promising promoters fall into two classes: (1) nonreducible metal oxides, such as CaO, K<sub>2</sub>O, Al<sub>2</sub>O<sub>3</sub> and MgO, and (2) partially reducible metal oxides which can be classified as co-catalysts, such as oxides of Mn, Mo, Ce, La, V, Re and rare earths. Possible catalyst supports include zeolites, alumina, silica, magnesia and high area carbons. Methods of producing active supported iron catalysts for CO hydrogenation will be investigated, such as development of shape selective catalysts which can provide control of product distribution. In view of the importance of temperature, alternative reactor systems (to fixed bed) will be investigated to attain better temperature control. Conditions will be used which give predominately lower molecular weight liquids and gaseous products.

#### Task 14 Characterization of Catalysts and Mechanistic Studies

Catalysts which show large differences in selectivity in Task 13 will be characterized as to surface and bulk properties. Differences in properties may provide the key to understanding why one catalyst is superior to another and identify critical properties, essential in selective catalysts. Factors relating to the surface mechanism of CO hydrogenation will also be investigated. Experiments are proposed to determine which catalysts form "surface" (reactive) carbon and the ability of these catalysts to exchange C and O of isotopically labelled CO. Reactions of CO and H<sub>2</sub> at temperatures below that required for CO dissociation are of particular interest.

#### Task 15 Completion of Previously Funded Studies and Exploratory Investigations

This task is included to provide for the orderly completion of coal liquefaction research underway in the expiring University of Utah contract, EX-76-C-01-2006.

### III Highlights to Date

Studies on the basic properties of supported sulfide catalysts showed that different supports have a profound influence on catalytic activities of CoMo catalysts. The three functions of hydrodesulfurization, hydrogenation and cracking were differently affected depending on the support used and the manner of preparation of the catalyst. Also, incorporation of additives to the support showed that the different catalytic functions can be selectively affected.

A systematic study concerned with catalytic cracking of coal-derived liquids, viz., an SRC-II middle-heavy distillate and four hydrotreated SRC-II products was carried out in the range of 375 - 500°C (LHSV, 0.2 - 3.9 hr<sup>-1</sup>). Hydrotreatment, even to a limited extent, results in a remarkable improvement in the yield of gasoline-range products from the SRC-II distillate. This improvement is ascribed to: (a) hydrogenolysis reactions leading to lower molecular weight feedstock components and (b) limited hydrogenation of aromatic rings leading to polycyclic feed components with sufficient concentration of hydroaromatic rings needed for effective cracking. The results with model compounds and the data on hydrogen consumption during hydrotreatment of SRC-II liquids indicate that for tricyclic, tetracyclic, and pentacyclic coal-liquid components the optimal concentration of hydroaromatic rings for effective subsequent cracking is at least two rings per molecule.

#### Papers and Presentations

1. R. Pugmire, "Structural Characterization of Coal Macerals Using <sup>13</sup>C CP/MAS Techniques," presented at the Gordon Research Conference, New Hampton, New Hampshire, June 30, 1980.

## Task 2

### Carbon-13 NMR Investigation of CDL and Coal

Faculty Advisor: R.J. Pugmire  
Post-Doctoral Fellow: D.K. Dalling

#### Introduction

The work carried out over the last several months has focused on three aspects of the application of CP/MAS (cross polarization, magic angle spinning) NMR to fossil fuels. The first and most extensively investigated area has been in the development of probes and rotors to increase the sensitivity and ease of experimentation without sacrificing resolution or spinning speed. The second area has been an assessment of the reliability of quantitative results obtained from CP or CP/MAS experiments. Thirdly, the technique has been applied to two well characterized western whole coals at this time.

The initial work on the analysis of coal-derived liquids obtained from 24 producing Utah coal mines has also been completed.

#### Project Status

The probe and magic angle spinner previously<sup>1</sup> developed in this laboratory have served as the starting point for furthering the state-of-the-art in this field. Several aspects of this design make it very useful for routine examination of fossil fuels.

A unique aspect of this probe is that the sample may be removed without having to remove the probe from the magnet and a new sample inserted without having to readjust the magic angle. Samples of 150 mg can be routinely spun at speeds  $\geq 4.0$  KHz making sideband free operation possible in 23 kg magnetic fields. In most instances this experimental set-up is optimum, especially if one is sample limited. However, in the analysis of fossil fuels, one is usually not sample limited. If a larger sample can be spun, the greater sensitivity realized will be translated into increased sample throughput. While a spectrum can be observed in  $\sim 2000$  scans (1.7 hr) on 150 mg samples, it is best to collect 10 to 25 thousand scans (8 to 20 hr) for sufficient signal to noise to allow resolution of differing chemical types. With this in mind, a probe and spinner system is being developed that is capable of spinning samples of 500 mg or more at rates over 6 KHz. This will represent at least a three-fold increase in sensitivity over the current probe with an associated order of magnitude savings in time.

The basic difficulty associated with the CP/MAS experiment is in spinning the sample fast enough to reduce the spinning sidebands to less than a few percent. This is illustrated well in a comparison of the spectra of 9 methyl, 9-10 dihydroanthracene taken at two different magnetic fields and spinning rates (Figure 1). The upper spectrum is taken

at 25 MHz for  $^{13}\text{C}$  and at a spinning rate of approximately 5 KHz. The sidebands are nearly imperceptible and are located well out into the wings of the spectra. In the lower trace, taken at 50 MHz for  $^{13}\text{C}$  and at a spinning rate of 1.5 KHz, the spectrum is dominated by the sidebands, which go up to the fourth order. Furthermore, the intensity of the sidebands have an asymmetry of approximately 50% representative of the nature of the chemical shift tensors. At this field strength, in order to provide a sideband free spectra of comparable quality to that obtained at 23 kg, one would require 10 KHz sample spinning rate.

As a rule of thumb, the minimal useful spinning rate needed for  $^{13}\text{C}$  CP/MAS spectroscopy must be equal to or greater than 150 ppm at the field being used, and a value of 200 ppm is preferred to assure the absence of overlap of spectral lines and sidebands in many substances. Experience has shown that spinning at this rate will generally reduce the sidebands of the aromatic and carbonyl carbons to <10% of the total intensity and push the upfield sideband on the upfield side of the aliphatic carbons. The following are ranges of necessary sample rotation rates at illustrative field strengths:

Magnetic Field of	Range of Spinning Rates Needed
14 kg (15 MHz for $^{13}\text{C}$ )	2250 - 3000 Hz
23 kg (23 MHz for $^{13}\text{C}$ )	3750 - 5000 Hz
46 kg (50 MHz for $^{13}\text{C}$ )	7500 - 10000 Hz

The general multi-purpose NMR spectrometer of the immediate future is evolving as an instrument based on a 46 kg superconducting solenoid and, as such, the ability to spin at speeds of at least 7500 Hz is needed to make the CP/MAS technique practical at these field strengths. In many cases the extra dispersion afforded by higher fields reveals more structural information and is accompanied by greater sensitivity. (Sensitivity increases approximately as the  $3/2$  power of the field strength.) Line-widths do however often scale with field if they are dominated by the spread of susceptibilities seen by the resonant nuclei, and in this case no additional resolution is realized at higher fields. Generally, some fraction of the gain in dispersion is realized. A comparison of the spectra taken at 25 and 50 MHz for  $^{13}\text{C}$  of 9,9,10 trimethyl-9,10 dihydroanthracene is typical (Figure 2). Although the extra resolution is not a full factor of two, one does observe an improvement of approximately  $1/3$ .

For a sample of 500 mg, the problem now is how to rotate the samples at a minimum rate of 7500 Hz. A sample  $1/4$  in. in diameter and  $5/8$  in. tall ( $0.5 \text{ cm}^3$ ) has been chosen. A material rotor geometry must now be chosen. In this problem there are two design criteria.

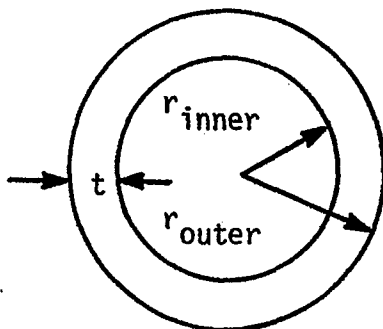
1. The speed at which the rotor spins is limited by the speed of sound in the driving medium. It is usually practical to spin at a rate at which the periphery of the maximum diameter of the rotor has a tangential velocity of about  $2/3$  the speed of sound in the medium.
2. The tensile strength of the material must be high enough to take the tremendous centripetal forces generated at these rates. A further requirement is that the material must also not produce a large background in the CP/MAS experiment.

Since spinning will be done with compressed air (speed of sound = 1140 ft/s), the maximum outer diameter of the rotor will be

$$7500 \text{ Hz} \times \pi D \text{ ft/cycle} = 2/3 (1140) \text{ ft/sec} \text{ or } D=0.39 \text{ in. or } \sim 10 \text{ mm}$$

To calculate the stress induced by the sample on the rotor, a simple model will be used including only the hoop stress in the walls to obtain the stress due to the sample ( $\sigma_s$ )

$$\sigma_s t = r P_s$$



$\rho_s$  is the pressure at  $r$  produced by spinning the sample (assuming a thin wall cylinder, i.e.,  $r > 5t$  where  $t$  is the wall thickness).

Now

$$P_s = \rho_s \frac{\omega^2 r^2}{2}$$

where  $\rho_s$  is the sample density and assumes the sample is fluid like.

Assuming a density of  $\sim 1.0$  g/cc,  $P_s$ , at 7500 Hz with  $r=0.125$ ", is  $\sim 1600$  psi or  $\sigma_s t = 200$  psi-in.

The mass of the rotor will also contribute to the stress in the walls in a more complex fashion. For this estimate a wall thickness of 0.050" will be used giving equal volumes of rotor material and sample in the coil. For  $\rho$  the average of the sample (1.0 g/cc) and the rotor material will be used. This increases the effective  $r$  to a value of  $(r_{outer} + r_{inner})/2$ . For the wall thickness of 0.050" and an O.D. of 0.350", the average  $r$  is 0.150". Thus

$$\sigma_{total} t \sim 350 \text{ psi in} \quad \text{or} \quad \sigma_{total} = 7000 \text{ psi} \quad (\rho_{average} = 1.0)$$

Unfortunately this is at the limit of the strength of most plastics.

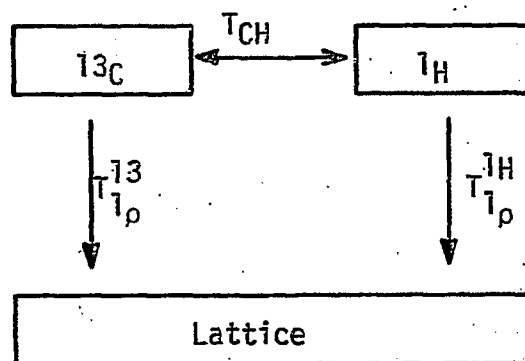
Listed in Table 1 are a number of materials tried with advantages and disadvantages.

As noted in the Table, Delrin is the only material used to date that is suitable for rotation of  $>7500$  Hz with this rotor design. The deuterated PMMA, Boron nitride and Kel-F have little or no background but do not wear well as rotors. Below 5 KHz, Kel-F is adequate but deforms at higher rates. Boron nitride exhibits excessive wear due to the starting and stopping of the rotor and is not serviceable. The deuterated PMMA, in theory, should be able to go to  $+7000$  Hz but because of its low impact strength, hairline cracks develop from starting and stopping the rotor and from machine fabrication. The cracks eventually weaken the rotor until it explodes violently when rotating. Unfortunately, even though the  $^{13}\text{C}$

signal from Delrin is only a single line, it can be so intense that in a long run, as with fossil fuel samples, it can be difficult to separate it from the spectrum. Currently, the possibility of having deuterated Delrin made for this application is being investigated as it should give no background in the spectra. The outside development of glass fiber reinforced Kel-F is actively being pursued as another possibility for a rotor material.

While  $^{13}\text{C}$  CP/MAS spectroscopy is recognized as one of the best methods for characterizing the carbon functionalities present in fossil fuels, there is always the question of quantitation of results. Are all the types of carbon present in coals observed and is there any differential discrimination in the cross polarization process? To begin to answer some of these questions, a limited set of CP data has been taken on a model compound, hexamethylbenzene (HMB), and on two of the coals studied under this contract. The preliminary findings will be discussed.

First, consider the problems in quantifying the CP experiment.



Consider the above thermodynamic model of the cross polarization process. Under spinlocking of the  $^1\text{H}$ 's in the sample and simultaneous irradiation of the  $^{13}\text{C}$  under the Hartmann-Hahn condition, magnetization is transferred from the  $^1\text{H}$ 's to  $^{13}\text{C}$  at a rate characterized by  $1/T_{\text{CH}}$ . This rate depends on the strength of the dipolar interaction between the  $^{13}\text{C}$  and its nearest neighbor  $^1\text{H}$ 's. In a system as heterogeneous as a coal, there will be a large range of  $T_{\text{CH}}$ 's, short for groups such as methyls and other protonated carbons and longer for  $^{13}\text{C}$ 's isolated in the interiors of condensed aromatic rings. Thus, for short polarization times one might expect to preferentially enhance the signals due to groups such as methyls, methylenes and methines. To avoid this problem, long cross polarization times might be used. However, the problem is complicated by other relaxation processes. To fully polarize the  $^{13}\text{C}$  in the sample, the rate  $1/T_{\text{CH}}$  must be much faster than the rates  $1/T_{1\rho}^{13\text{C}}$  and  $1/T_{1\rho}^{1\text{H}}$  which characterize how fast the spinlocked magnetizations relax away from the applied radio frequency fields. If  $1/T_{\text{CH}}$  is much slower than  $1/T_{1\rho}^{1\text{H}}$  or  $1/T_{1\rho}^{13\text{C}}$ , no carbon magnetization will occur due to the cross polarization process. If  $T_{\text{CH}}$  is comparable to the  $T_{1\rho}$ 's, the competing rates will dictate a mixing time that will be optimum for data acquisition. Again, in a heterogeneous system like coal, there will be a range of these rates, and the possibility exists that one type of  $^{13}\text{C}$  may not be polarized as efficiently.

To determine how these problems can affect the CP response of fossil fuels, the behavior of two coals was compared to that of a well characterized model compound, HMB. In Figure 3, the total intensity in arbitrary units per gram of carbon is plotted for the three samples vs. mixing time. HMB polarizes quite rapidly and between 0.1 msec to  $\sim 1.0$  msec increases exponentially in signal intensity with full relative intensity observed for polarization times in the 1.3 msec range. At times longer than 3 msec, however, the proton  $T_{1\rho}$  processes start to appreciably destroy the  $^1\text{H}$  magnetization, and the  $^{13}\text{C}$  magnetization is lost back to the decaying proton reservoir along with some decay caused by the  $^{13}\text{C}$   $T_{1\rho}$  processes.

In Figure 4 the value of  $f_a$  is plotted vs. mixing time. For HMB the quick rise to a steady state value of about 0.55\* shows that, although the  $\text{CH}_3$ 's may polarize faster than the aromatic carbons, the rate  $1/T_{\text{CH}}$  for both types of carbon is much faster than either  $T_{1\rho}^{\text{H}}$  or  $T_{1\rho}^{13\text{C}}$ . This is borne out by the fact that at long mixing times, even though the total signal is decreasing, both aromatic and aliphatic carbon decrease at the same rate, i.e.,  $f_a$  is constant. As shown in Figure 4, the  $f_a$  value has maximized for HMB when a mixing time of approximately one msec is employed.

The spectral response for HMB will be compared with the accompanying composite curves for the Hiawatha and New Mexico coals. On the total magnetization curve (Figure 1), both coals behaved similarly, although the maximum signal response was observed at slightly shorter mixing times. At mixing times less than 1 msec, both coals polarize at rates comparable to HMB, indicating similar  $T_{\text{CH}}$ 's for these coals and HMB. However, the full enhancement for the coals is not realized at the maximum ( $\sim 1$  msec) response time and the relative spectral intensity for the coals is only about 70% to 80% of that obtained for HMB and drops off at a more rapid rate than that observed for HMB. This is a reflection of shorter  $^1\text{H}$   $T_{1\rho}$ 's for the coals. Thus the magnetization starts to decay at shorter times for the coals and never reaches the full value obtained for HMB. However, as shown in Figure 4, it is again noted that  $f_a$  rapidly reaches a steady state indicating, for the carbons observed, that the  $T_{1\rho}$ 's involved in the decay are similar for both types of material and as such is probably dominated by the proton  $T_{1\rho}$ 's. Thus, for mixing times of 1 msec or greater, the  $f_a$  values accurately reflect 70-80% of the basic carbon structure for these two coals.

Figure 5 displays the response to mixing time of the aromatic carbons in HMB and the two coals studied. Within experimental error, the response behavior is similar to that observed in Figure 3 for all carbons and suggests no differential discrimination in the detection of aromatic and aliphatic carbons.

The preceding discussion leaves two basic questions to be answered. Is the 70% to 80% of the carbon observed basically the same as that not observed, or are certain types of carbon being discriminated against? Why can only this amount of carbon be seen?

\*The difference between 0.55 measured  $f_a$  and the theoretical value of 0.50 is due to the manner in which the integration was done in this preliminary data and is a systematic baseline definition problem. This weights the results toward the more aromatic side as the data taken was nonspinning. This problem will be systematically investigated soon.

The last question has been partially answered by Gerstein and co-workers? They have observed relaxation phenomena in the broadband proton spectra of coals characteristic of a double exponential, indicating two types of protons exhibiting very short ( $\sim 100\mu\text{s}$ ) and a longer (msec)  $T_{1\rho}$ . Undoubtedly the protons with the short  $T_{1\rho}$ 's could account for neighboring carbons not being polarized effectively and according to Gerstein, could account for 10% to 30% of the  $^{13}\text{C}$  not being polarized. This observation is consistent with this laboratory's preliminary data. Thus part of the reduction in intensity is because some carbons experience very little spin polarization. This is in addition to the observation that protons with large values of  $T_{1\rho}$  do not efficiently polarize the adjacent carbons. Why some  $T_{1\rho}$ 's are so much shorter is not known, but it may be due to the presence of localized paramagnetic centers in the coals.

The first question has yet to be resolved. Given that the lost  $^{13}\text{C}$  magnetization is most likely due to the protons with much shorter  $T_{1\rho}$ 's, the identification of these protons, i.e., aliphatic vs. aromatic, would tell if any one type of  $^{13}\text{C}$  were being preferentially burned out of the spectrum. In principle, this should be possible to do by indirectly monitoring the  $T_{1\rho}$  relaxation of the protons via the  $^{13}\text{C}$  to which they are attached and thus separate them into aliphatic or aromatic types. The data in Figure 5, however, indicates that the loss in aromatic signal is similar in magnitude to that observed when considering all carbon. Furthermore, the effect of paramagnetic species on the CP process is to be investigated by doping model hydrocarbons such as HMB with controlled amounts of stable free radicals to check the validity of the paramagnetic induced proton relaxation hypothesis. By doping model hydrocarbons to the same level as determined by ESR spin counts on whole coals, the same behavior in the model compounds as in the coals should be reproduced.

While the data set collected thus far is limited, it does raise hope that the technique may be more quantitative than it may first appear. A similar analysis needs to be carried out on a number of coals varying widely in rank, petrographic composition and aromaticity. For the two coals investigated so far, 70% to 80% of the carbons observed is likely to be representative of the entire coal, provided the protons with short  $T_{1\rho}$ 's are uniformly distributed throughout the coal. In light of the proton relaxation data in the literature on coals and these data, the amount of  $^{13}\text{C}$  not being observed may be due to the region in the coal characterized by short  $T_{1\rho}$ 's and not due to inefficient carbon spin polarizations in extensive proton free regions (i.e., large condensed aromatic rings). In either case, the reactive matter (nongraphite like) is probably better characterized in a quantitative sense by the CP experiment than had been speculated. These tentative conclusions will hopefully be further substantiated by the experimental work to be undertaken as a future part of this contract.

The spectra have been taken for all coal-derived liquids obtained from the 24 producing Utah coal mines. The  $^{13}\text{C}$  NMR spectra exhibit general similarities for all the coal-derived liquids. The coals that have low conversion efficiencies ( $\sim 60\%$ ) exhibit modest structural variations in the aromatic region, but all samples have essentially identical structural features in the aliphatic region. Furthermore, all  $f_a$  values cover a narrow range (0.51 - 0.55).

### Future Work

In addition to the future work already outlined, the following studies will be initiated next quarter:

1. The liquids obtained from coals that have low conversion efficiencies will be re-examined. In particular, chemical shift reagents will be used to aid in the analysis of this complex aromatic region. The results of this work will be compared with similar data obtained on a CDL obtained from a coal with high conversion efficiencies.
2. The coals, using CP/MAS techniques, from which each CDL was obtained will be examined. Also, the unreacted char will be examined for comparing structural characteristics found in the solid, liquid, and solid residue.

### References

1. K.W. Zilm, D.W. Alderman and D.M. Grant, J. Mag. Resonance, 30, 563 (1978).
2. B.C. Gerstein, Ames Laboratory, Department of Energy, private communication, April 1980.

Table 1

Material	$\sigma$ (psi tensile)	$\rho$ (g/cm <sup>3</sup> )	$\omega_r$ maximum calculated for $\frac{1}{4}$ " sample, .05" wall	$\omega_r$ by experiment	Advantage	Disadvantage
Delrin	10,000	1.4	8500 Hz	> 7500 Hz No break	Only one spectral line at ~ 80 ppm, takes high speeds, wears well.	Single line can become too large in spectrum.
Deuterated PMMA	7,000	1.2	7500 Hz	~ 5000 Hz	Can be deuterated to limit background.	Low impact strength, short rotor life.
Boron Nitride	Not Available	2.0	-	~ 4,500 to 6,000 Hz	No background.	Too soft - wears easily.
Kel-F	4,500	2.1	4900 Hz	Deforms at 5,000 Hz	No background.	Deforms easily.

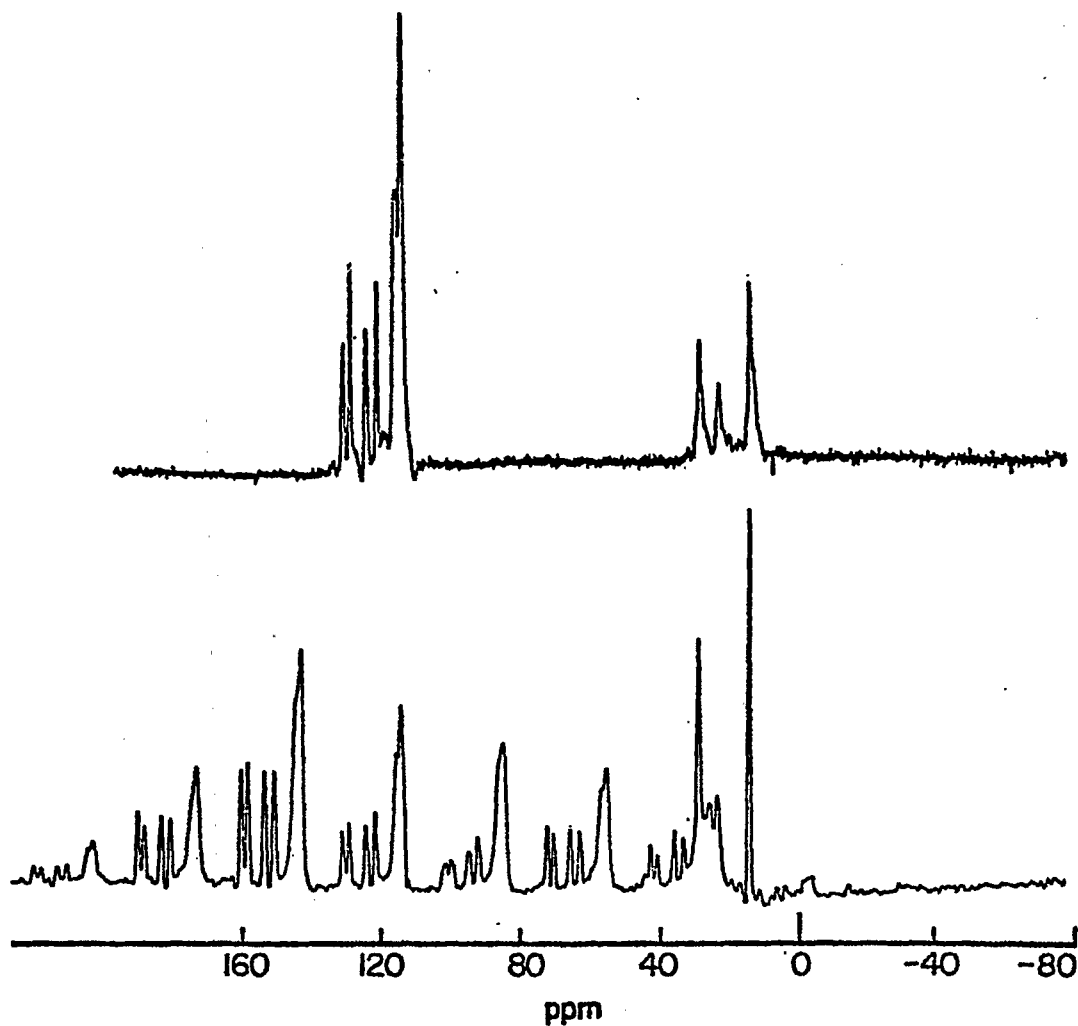


Figure 1. CP/MAS spectra of 9-methyl-9,10-dihydroanthracene.

- a) Data taken at 25 MHz with sample rotation rate of approximately 5 KHz.
- b) Data taken at 50 MHz with sample rotation of approximately 1.5 KHz. The center band is located at approximately 115 ppm.

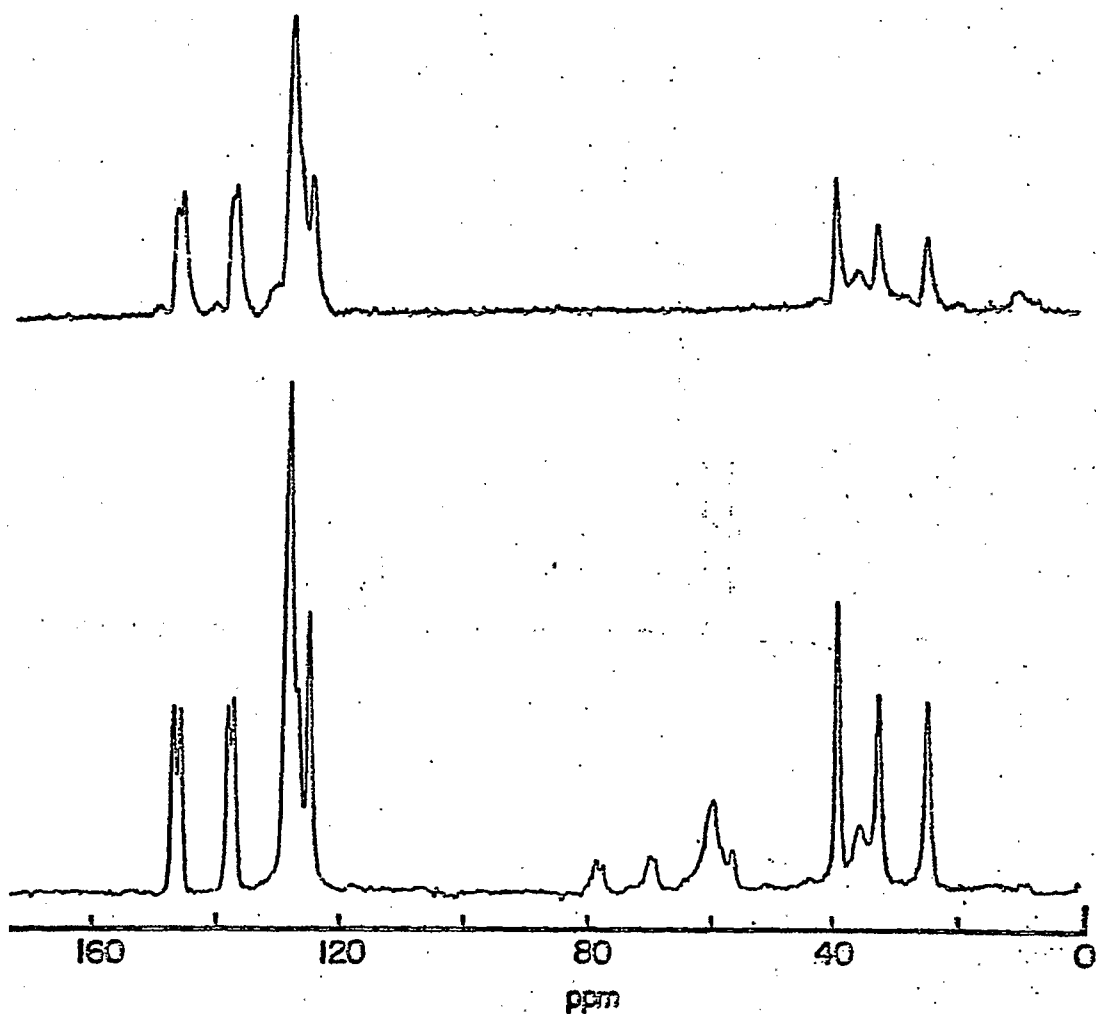


Figure 2. CP/MAS spectra of 9,9,10 trimethyl-9,10-dihydroanthracene.

a) 25 MHz with sample rotation rate of approximately 3 KHz.

b) 50 MHz with sample rotation rate of approximately 3.5 KHz.

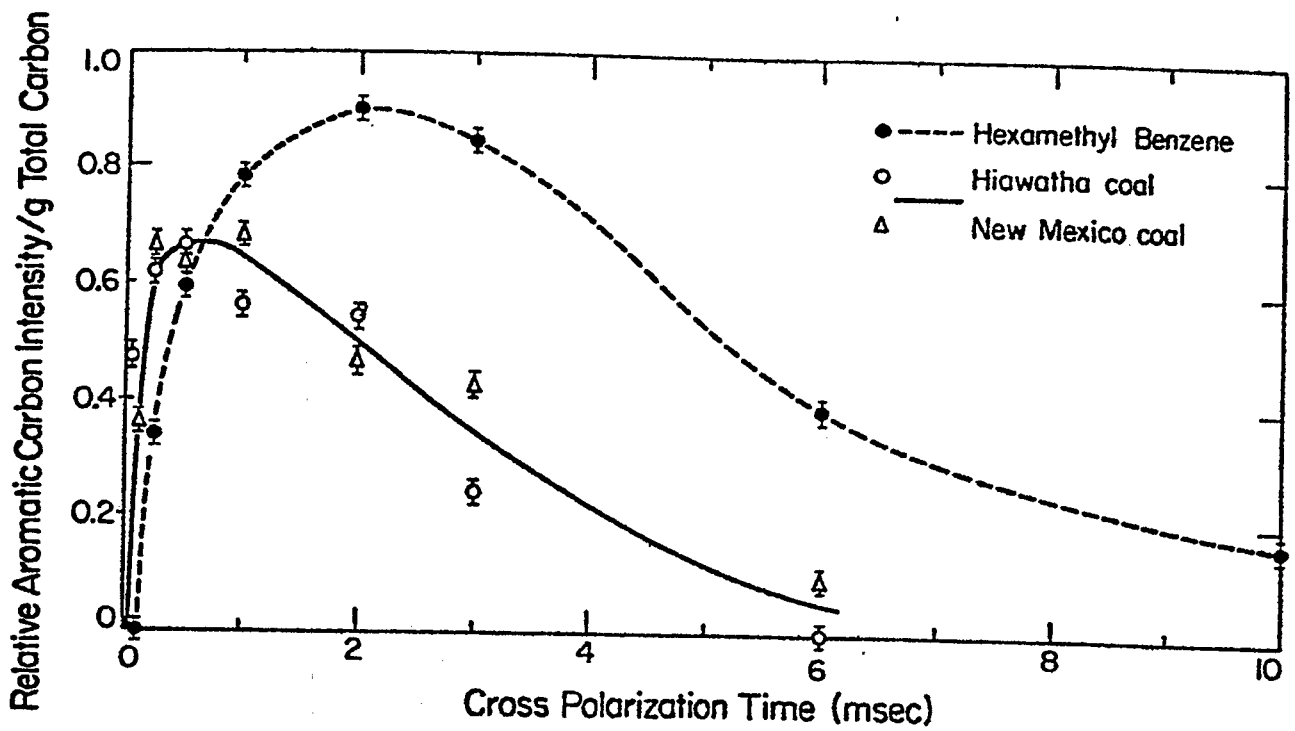


Figure 3. Relationship of cross polarization time and observed signal intensity.

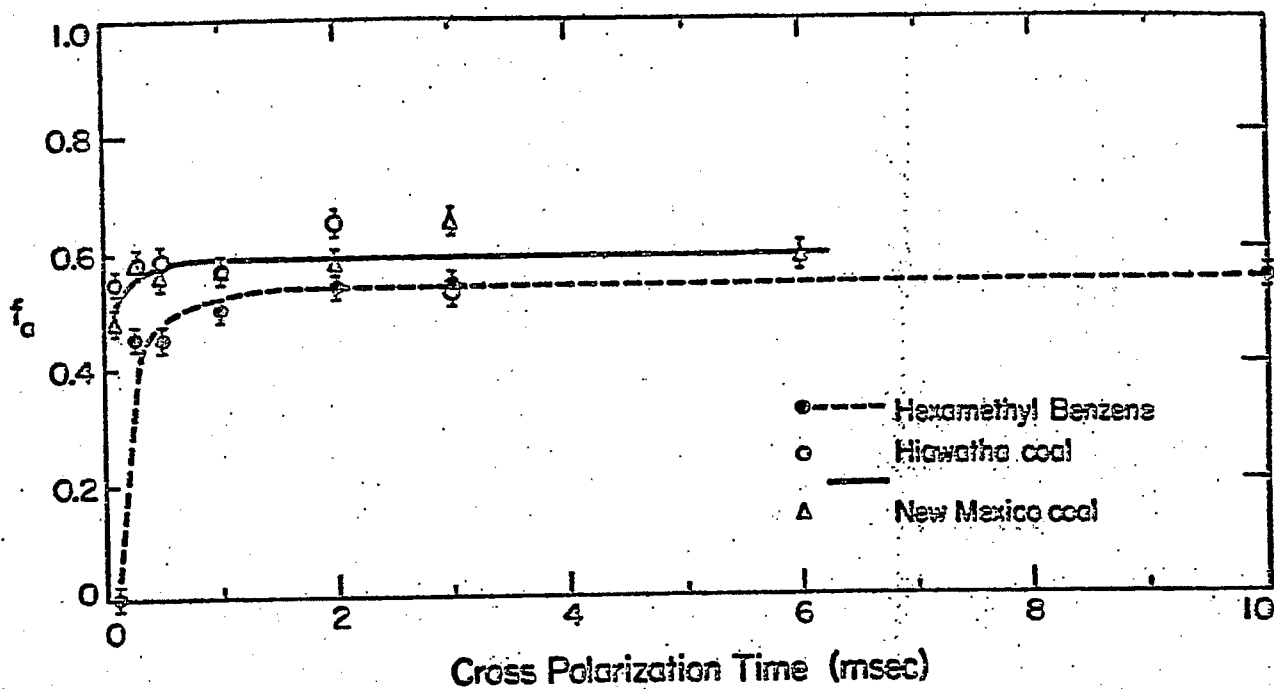


Figure 4. Relationship of  $f_a$  values to cross polarization time.

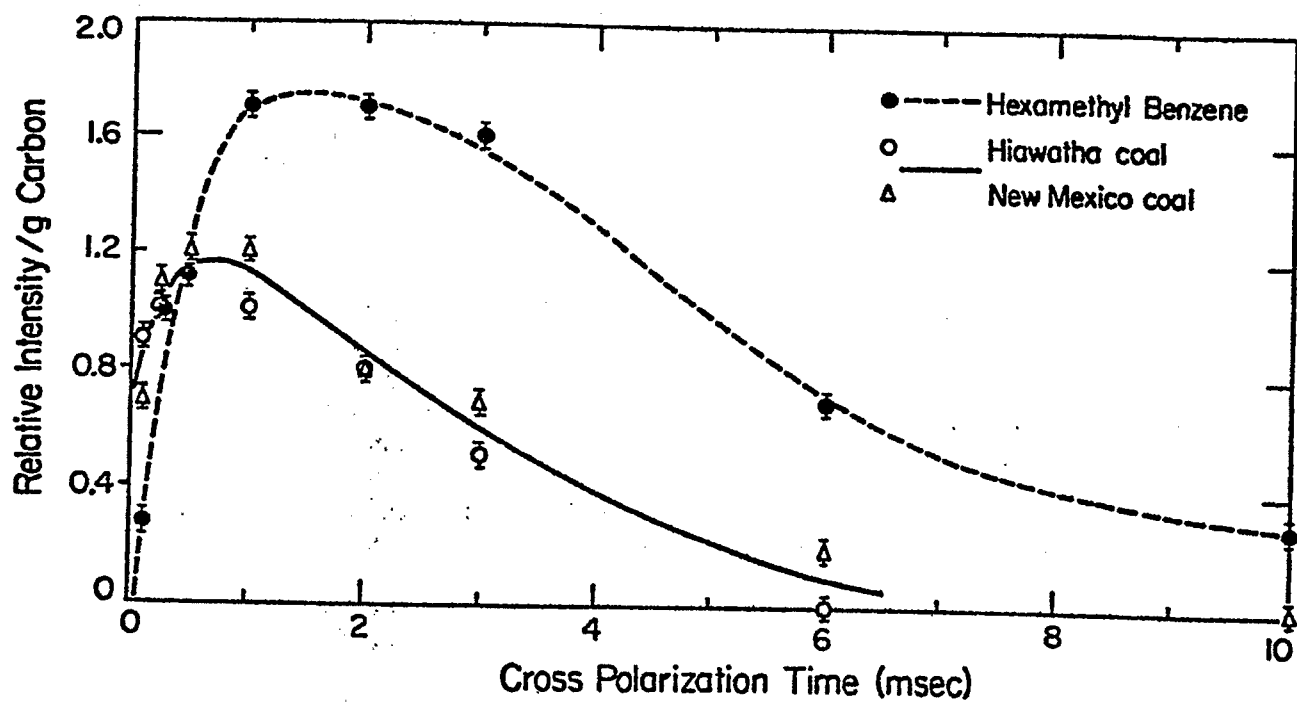


Figure 5. Response of aromatic carbons as a function of cross polarization time.

### Task 3

## Catalysis and Mechanism of Coal Liquefaction

Faculty Advisor: D.M. Bodily  
Graduate Student: Jason Miller

### Introduction

The hydroliquefaction of coal may be characterized by a mechanism which involves the initial rupture of covalent bonds to form reactive intermediates. These intermediates may be stabilized by hydrogen transfer to form lower molecular weight products or they may polymerize to form insoluble char or coke. Metal halides such as zinc chloride have been shown to be active in the bond scission stage of the reaction where as many catalysts are active only in stabilizing the intermediates, often by regenerating a hydrogen donor. The combination of thermal and catalytic reactions occurring simultaneously results in a complicated reaction mechanism. The chemistry of  $ZnCl_2$  will be studied with model compounds and coal by such reactions as hydrogen transfers, cleavage of specific bonds and interaction with  $\pi$  electron systems.

A high performance liquid chromatograph, HPLC, will be used to analyze liquid products of the reactions under study. Further characterization of the products will be by nuclear magnetic resonance, NMR, structural analysis and vapor pressure osmometry.

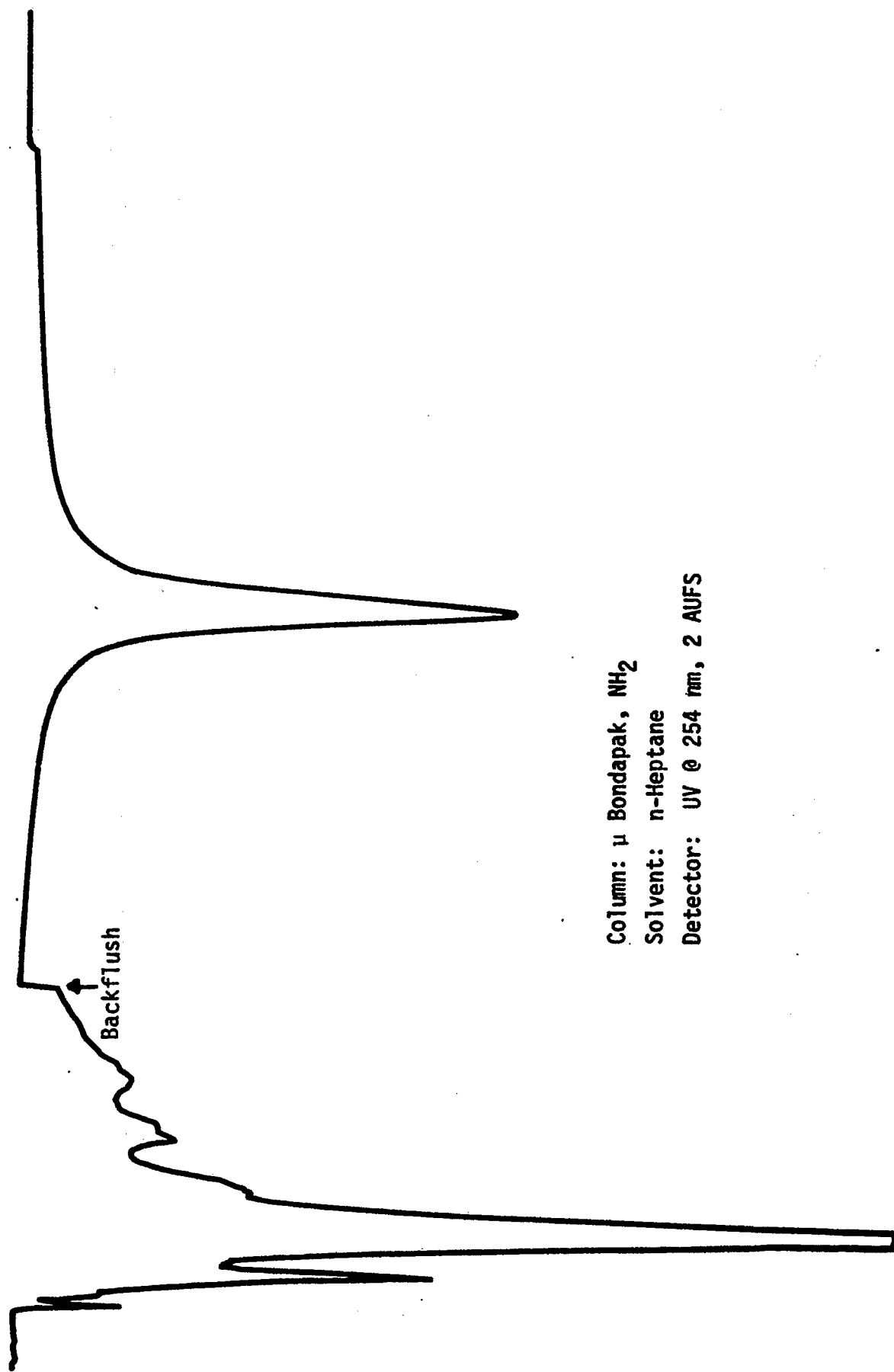
### Project Status

The hexane soluble portion of coal-hydrogenation liquids were separated on a  $\mu$ -Bondapack-NH<sub>2</sub> column into a nonpolar fraction and a polar fraction. A typical chromatogram for a sample obtained from Hiawatha coal is shown in Figure 1. The polar and nonpolar fractions were collected for further analysis. The nonpolar fraction was separated on a  $\mu$ -porasil column. The spectra for the Hiawatha coal liquid is shown in Figure 2.

### Future Work

The nonpolar fraction will be separated by reverse-phase chromatography using a phenyl column. Differences in liquids prepared from different coals will be studied.

Figure 1a. UV Chromatogram of Hiawatha coal liquid, hexane soluble.



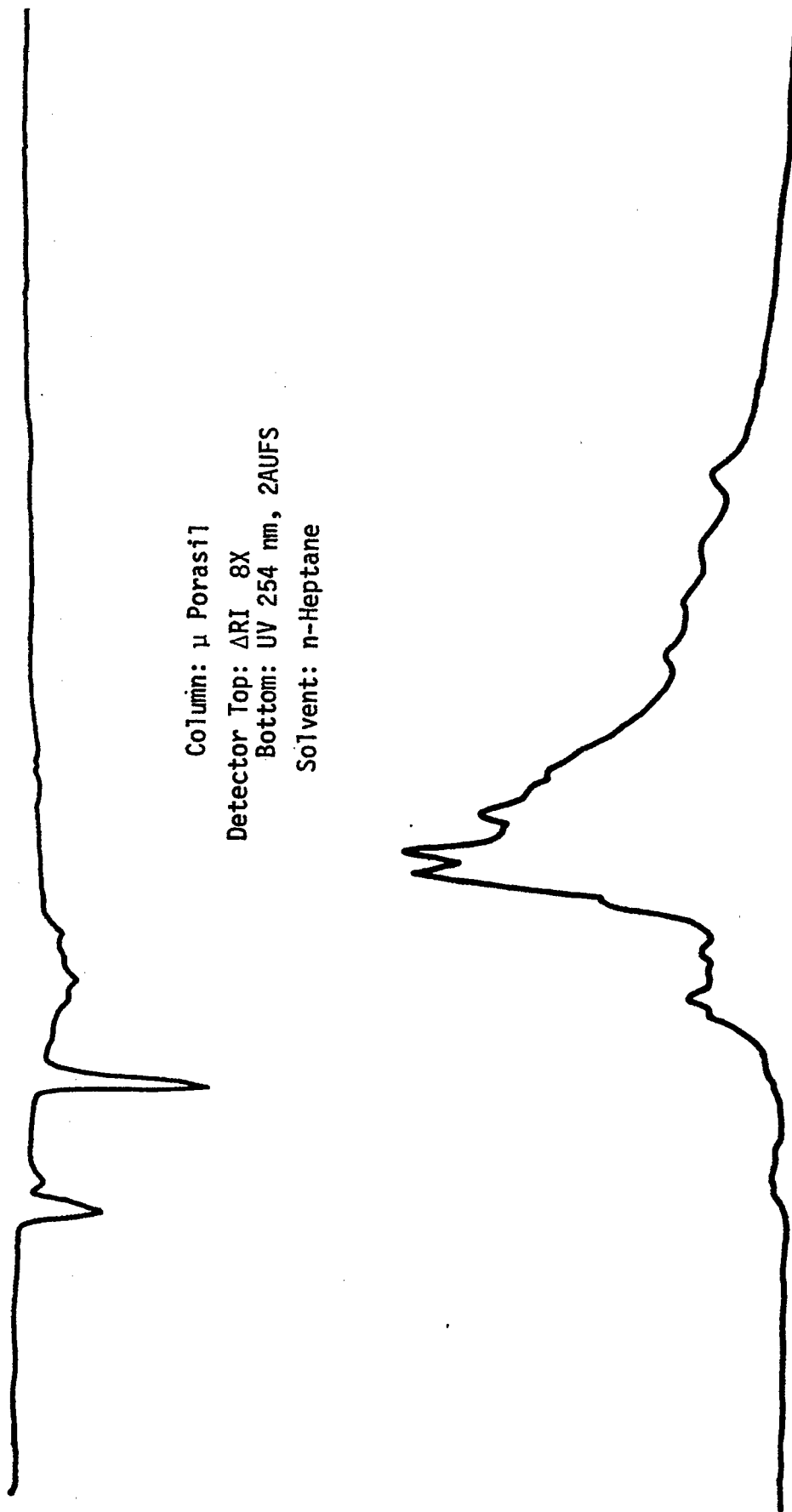
Column:  $\mu$  Bondapak, NH<sub>2</sub>  
Solvent: n-Heptane  
Detector: UV @ 254 nm, 2 AUFS

Figure 1b.  $\text{NH}_2$   $\mu$  Bondapak column, n-heptane solvent, Hiawatha coal, hexane soluble liquid.



Detector:  $\Delta$ RI 8X  
Column:  $\text{NH}_2$   $\mu$  Bondapak  
Solvent: n-heptane

Figure 2. Nonpolar fraction, hexane soluble Hiawatha coal liquid.



Column:  $\mu$  Porasil

Detector Top:  $\Delta$ RI 8X

Bottom: UV 254 nm, 2AUF5

Solvent: n-Heptane

## Task 4

### Momentum, Heat and Mass Transfer in Cocurrent Flow

Faculty Advisor: J.D. Seader  
Graduate Student: R. Sorenson

#### Introduction

This project concerns the momentum and heat transfer phenomena for gas/solid suspensions moving vertically upward through a tube. The solid is a 200 to 400 micron coal sample being transported by air.

#### Project Status

An error analysis of the equations used in calculation of the Fanning friction factor as applied here to experimental data showed that most error would be introduced by an inaccurate mass flowrate. The air feed rotameter was recalibrated after an air cooler was installed in the supply compressor. Some discrepancy was observed from the previously used relationship. The new calibration curve is shown in Figure 1.

Pressure drop runs for air alone were conducted at Reynold's numbers from 5000 to 30,000. Fanning friction factors were calculated and are shown in Figure 2. The resulting values are slightly higher than the widely accepted Nikuradse correlation for smooth tubes. The higher values can be explained by assuming that the stainless steel tube has slightly roughened walls. A relative roughness of only  $4 \times 10^{-5}$  is required to explain the variance from smooth tube behavior.

These same pressure drop results showed that between tube taps 4 and 5, and 11 and 12 an excessive pressure drop was present. Therefore, these sections of the tube should not be relied upon in further measurements, but since these same sections are at extreme ends of the column no adverse effects are observed in the steady-flow sections of the column.

Acceleration effects of air alone can be seen only in tap 1 and at higher flowrates in tap 2. There is a three-foot section of tube between the air inlet and the first tap where the air is accelerated, but if needed, this section could be tapped. Pressure drop across the entire column is at most 4 psi and density changes are negligible in the tube.

Test runs of air/coal particle mixtures were undertaken at solid mass load ratios (mass coal/mass air) varying from 0 to 15 at 7 different air mass flowrates. The pressure profiles were obtained for each run and representative data plots are displayed in Figures 3 and 4. The acceleration of the coal/air mixture is apparent here as can be seen by the increased pressure drops in the lower numbered taps. Of course, larger pressure drops were required to transport greater amounts of coal as can be seen in the figures.

Steady-state pressure drops were taken at taps 9 and 10 and 10 and 11. These two sets of taps gave repeated agreement (less than 0.05" H<sub>2</sub>O at loading ratios less than 10) over what amounts to a four-foot steady-flow test section. Figure 5 for the steady-flow test section shows steady-state pressure drops for load ratios of 0 to 10 for 3 different Reynold's numbers. Over this range, at least a linear behavior is observed between pressure drop and density of the fluid/particle mixture.

#### Future Work

The pressure drop for higher (12 to 18) loading ratios will be duplicated before being reported. The initial data show deviations from the linear behavior in Figure 5. Also, computer plots will be made of all the data not reported here in order to compare with the previously obtained downflow data. All fluid mechanics data has essentially been obtained but the higher load ratios are more difficult to obtain and are less reliable.

The size distribution of the coal particles was obtained initially. Once the high load ratio duplication runs are complete, the size distribution will be obtained again and compared with the original distribution.

The heat transfer section has been prepared and will be installed shortly. Computer programs will be written to obtain real-time temperature data from the heat transfer section.

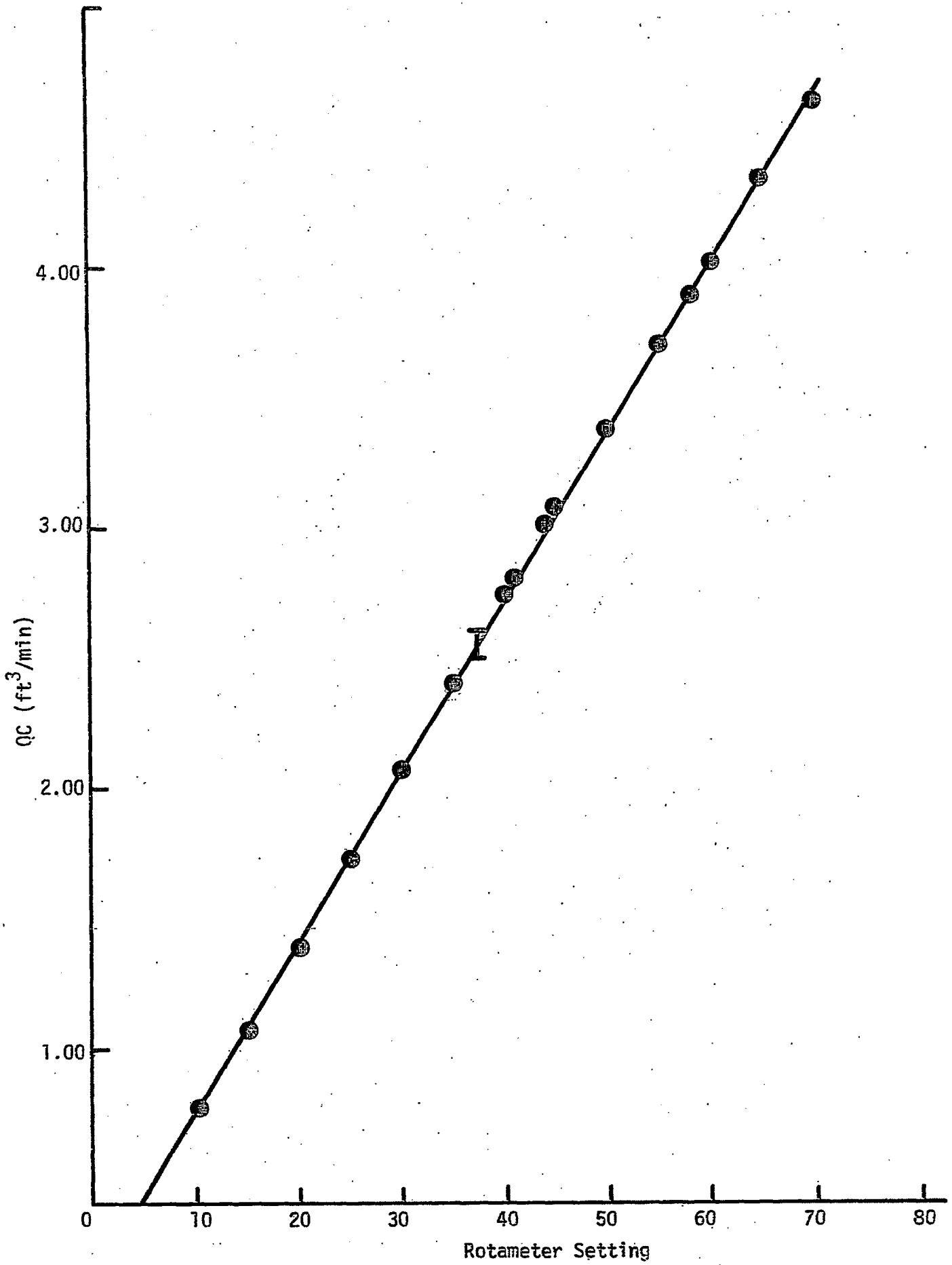


Figure 1. Calibration Chart.

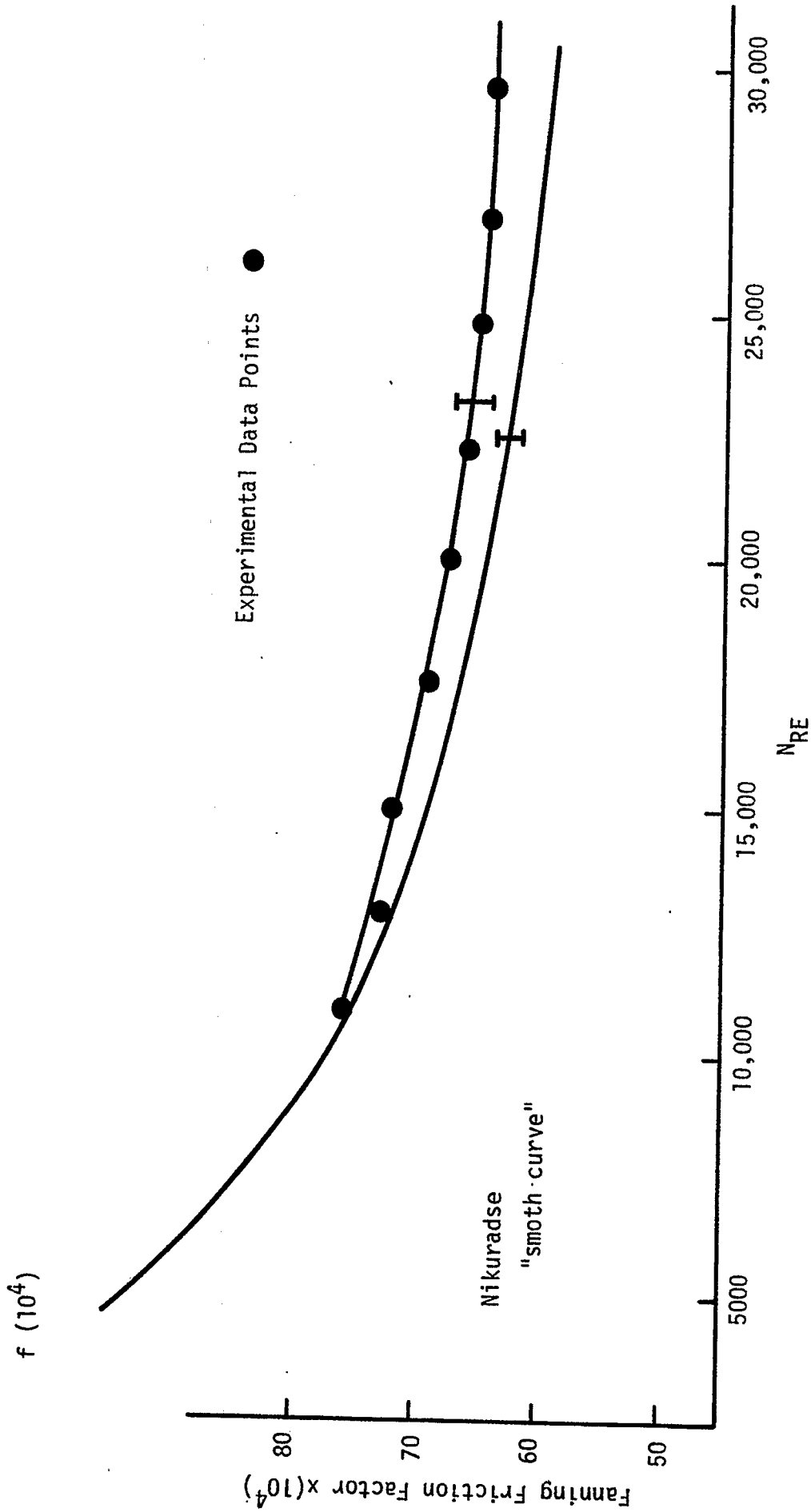


Figure 2. Experimental Friction Factors.

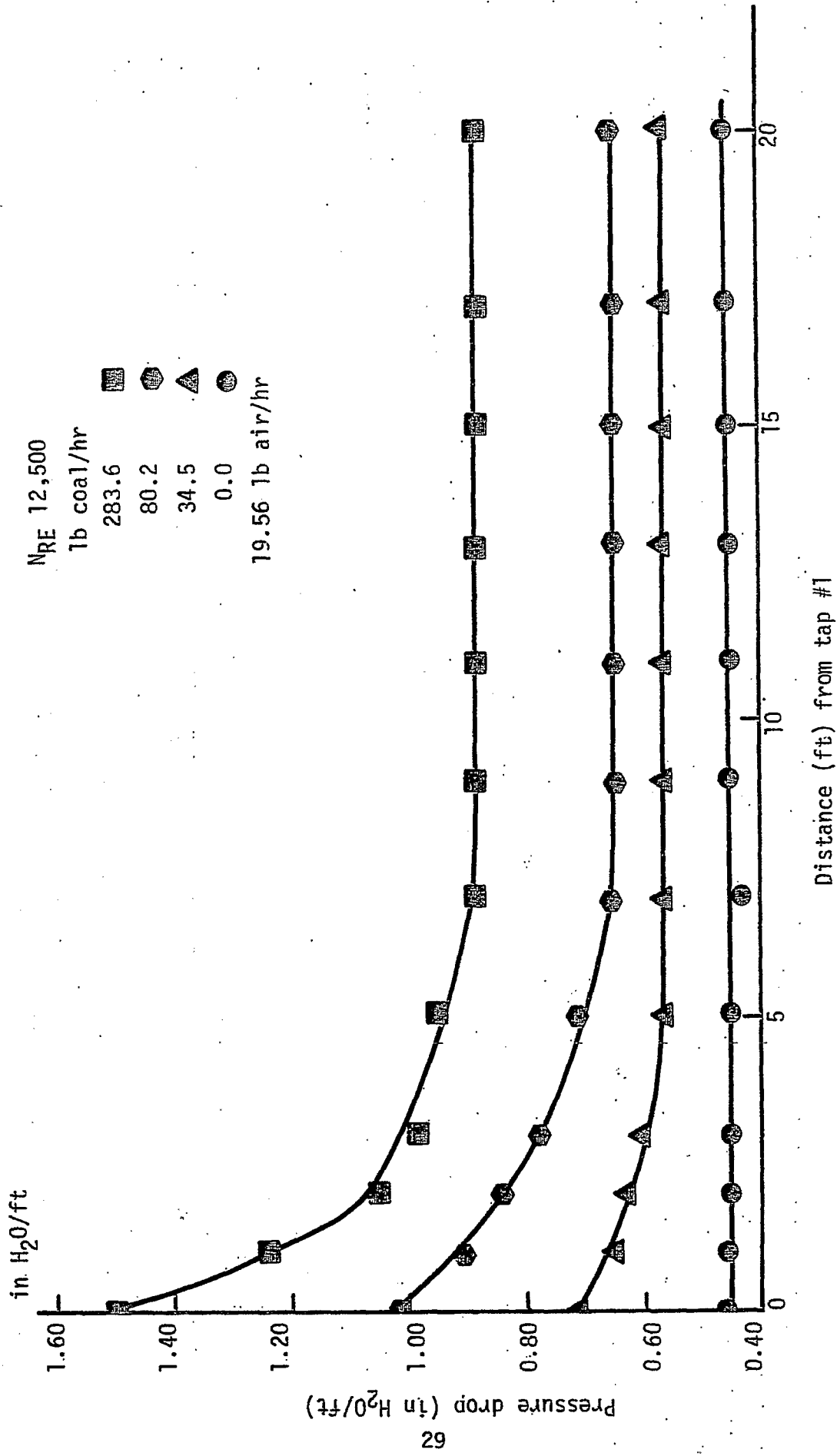


Figure 3. Pressure profiles at various loading ratios.

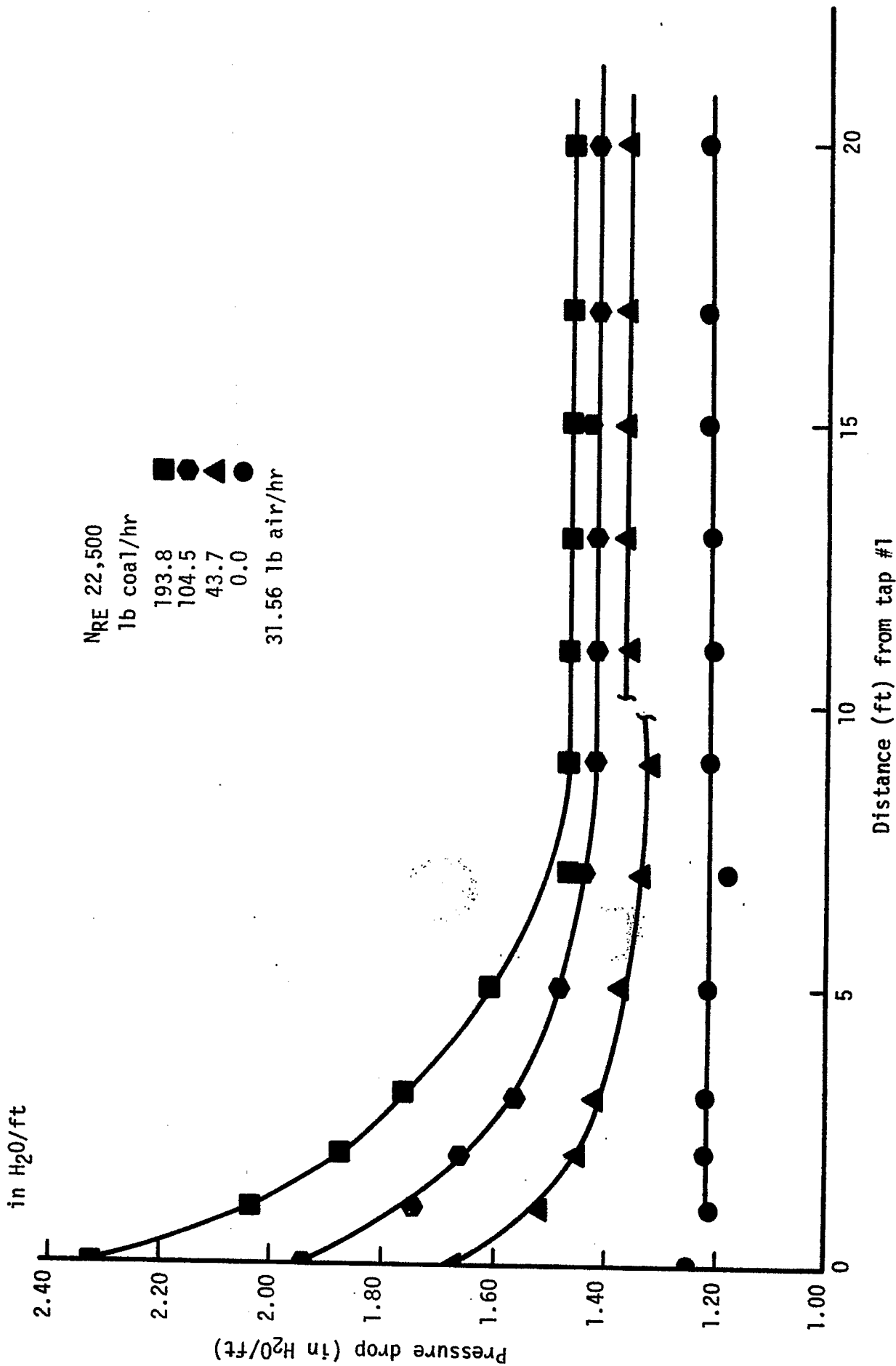


Figure 4. Pressure profiles at various loading ratios.

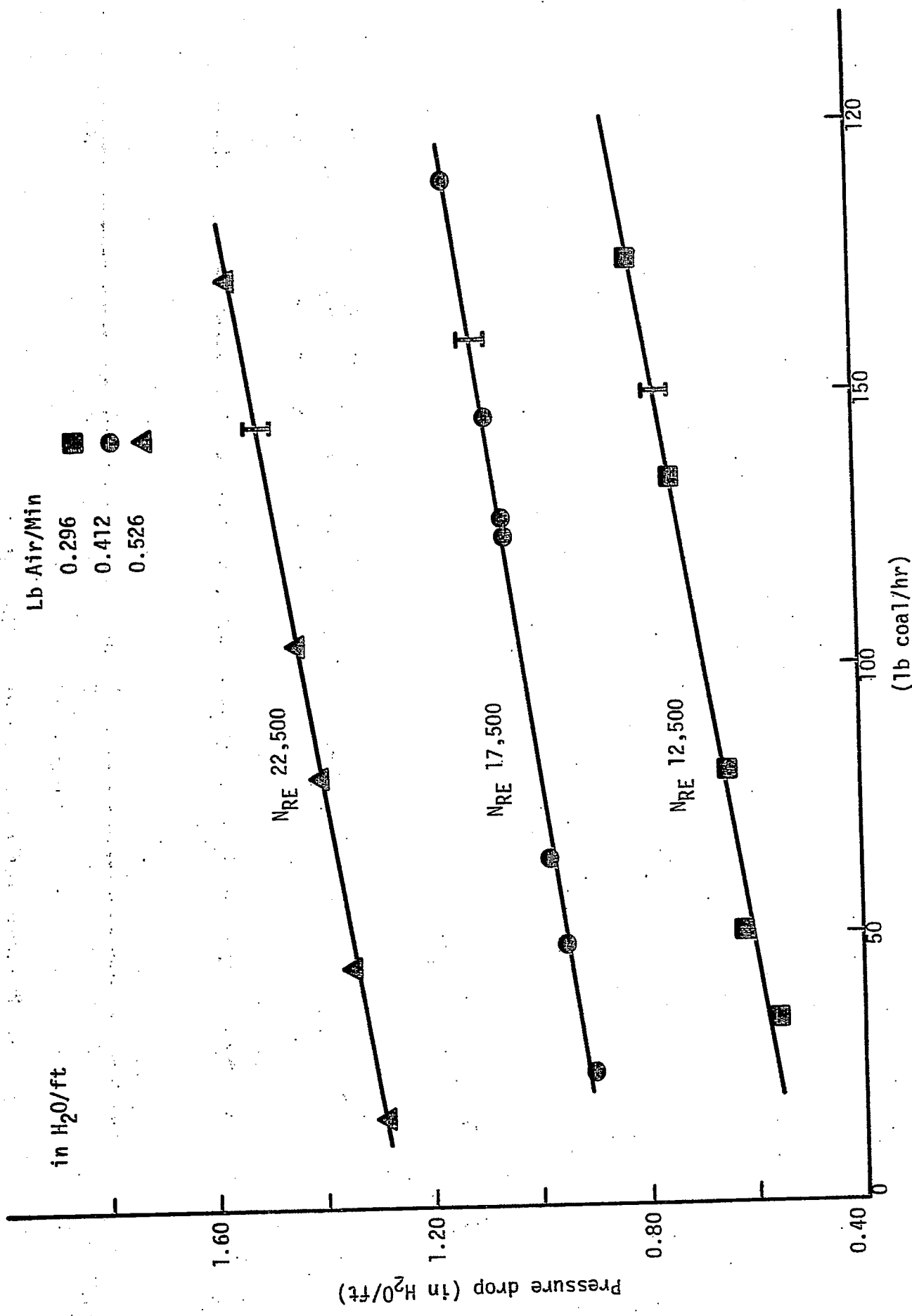


Figure 5. Pressure drop vs. coal flowrate.

## Task 5

### The Mechanism of Pyrolysis of Bituminous Coal

Faculty Advisor: W.H. Wiser  
Graduate Student: J.K. Shigley

#### Introduction

In the present state of knowledge concerning the fundamental chemistry of coal liquefaction in the temperature range 375-550°C, the liquefaction reactions are initiated by thermal rupture of bonds in the bridges joining configurations in the coal, yielding free radicals. The different approaches to liquefaction, except for Fischer-Tropsch variations, represent ways of stabilizing the free radicals to produce molecules. The stabilization involving abstraction by the free radicals of hydrogen from the hydroaromatic structures of the coal is believed to be the predominant means of yielding liquid size molecules in the early stages of all coal liquefaction processes, except Fischer-Tropsch variations. The objective of this research is to understand the chemistry of this pyrolytic operation using model compounds which contain structures believed to be prominent in bituminous coals.

#### Project Status

The pyrolysis apparatus has been assembled.<sup>1</sup> Test runs have been conducted to test the gas flow techniques, heat-up and cool-down times, sample injection mechanics and insulation efficiency. Extensive experience has been gained in sample preparation techniques, and a standard order of procedure has been developed so as to insure sample integrity, an inert atmosphere inside the tube with the sample and accurate measurement of the actual sample weight. Problems have been encountered with the plunger mechanism, sample tube sizes, sample collection and temperature control.

#### Future Work

More test runs will be made to find methods to improve the plunger mechanics, sample collection and temperature control. Once these problems have been adequately dealt with, experiments will be conducted at a series of temperatures from 300° to 450°C for various times to determine the kinetics and mechanisms of the model compounds pyrolysis. The literature search for related work will continue, also.

#### Reference

1. W.H. Wiser et al., DOE Contract No. DE-AC01-79ET14700, Quarterly Progress Report, Salt Lake City, Utah, Jan-Mar 1980.

## Task 6

### Catalytic Hydrogenation of CD Liquids and Related Polycyclic Aromatic Hydrocarbons

Faculty Advisor: J. Shabtai  
Research Associate: C. Russell

#### Introduction

The main objective of this research project is to develop a versatile process for controllable hydrotreating of highly aromatic coal liquids, viz., a process permitting production of naphthenic-aromatic feedstocks containing variable relative concentrations of hydroaromatic vs. aromatic ring structures. Such feedstocks, including the extreme case of a fully hydrogenated coal liquid, are suitable starting materials for catalytic cracking, as applied for preferential production of light liquid fuels.<sup>1,2</sup> The overall objective of this project and of a parallel catalytic cracking study is, therefore, to develop and optimize a hydrotreating-catalytic cracking process sequence for conversion of coal liquids into conventional fuels.

The present project includes also a study of metal sulfide-catalyzed hydrogenation of model polycyclic arenes present in coal liquids, e.g., phenanthrene, pyrene, anthracene and triphenylene, as a function of catalyst type and experimental variables. This part of the study provides basic information on the rate, mechanism and stereochemistry of hydrogenation of structurally distinct aromatic systems in the presence of sulfided catalysts.

#### Project Status

The present report is concerned with some initial results obtained in a study of the hydrogenation reactions of triphenylene (1) in the presence of a conventional sulfided Ni-W/Al<sub>2</sub>O<sub>3</sub> catalyst. Hydrogenation reactions were carried out in an autoclave system described elsewhere.<sup>3-5</sup> The experimental procedure was similar to that used previously.<sup>3-5</sup> Hydrogenation products were identified by a combination of gas chromatography-mass spectrometry, and by comparison with pure reference compounds.

With triphenylene (1) as feedstock, the product composition obtained under drastic hydrogenation conditions (temperature, 340°C; hydrogen pressure, 2600 psi; reaction time, 3 hr) was as follows:

<u>Product Component</u>	<u>% by wt</u>
1,2,3,4-tetrahydrotriphenylene (2)	46.1
1,2,3,4,5,6,7,8-octahydrotriphenylene (3)	17.2
1,2,3,4,5,6,7,8,9,10,11,12-dodecahydrotriphenylene (4)	28.8
perhydrotriphenylene (5)	7.9

Extension of the reaction time to 6 hr under otherwise identical conditions results in partial conversion of compound 2 into the more deeply hydrogenated products 3 and 4. However, there is relatively minor additional formation of perhydrotriphenylene (5). These results indicate that while the three peripheral aromatic rings in triphenylene (1) are hydrogenated at a fast rate, the residual central aromatic ring in the intermediate compound 4 is resistant to saturation even under drastic processing conditions. Examination of molecular models of 4, indicates that the hexasubstituted central ring would be prevented from easy flatwise adsorption on the catalyst surface, due to steric hindrance by the peripheral hydroaromatic rings.<sup>4</sup> This, in turn, could explain the resistance to exhaustive hydrogenation shown by heavy coal liquids, which contain various components with hexasubstituted aromatic rings.<sup>3</sup>

### Future Work

An autoclave has been modified allowing determination of kinetic rate constants for hydrogenation of coal liquids and of model polycyclic compounds. This autoclave system is presently being used in kinetic studies of condensed arenes, as well as of condensed heterocyclic-aromatic compounds. The stereochemistry of hydrogenation of model compounds is also being investigated. The study of the kinetics of hydrogenation of triphenylene will be completed.

### References

1. J. Shabtai, A.G. Oblad, W.H. Wiser and S. Sunder, DOE Contract No. E (49-18)-2006, Quarterly Progress Report, Salt Lake City, Utah, Jan-Mar 1979.
2. J. Shabtai, S. Sunder and A.G. Oblad, Preprints, American Chemical Society, Div. Petrol. Chem., Honolulu, Hawaii, Apr 1979, Vol. 24, p 653.
3. L. Veluswamy, Ph. D. Thesis, University of Utah, Salt Lake City, Utah, 1977.
4. J. Shabtai, L. Veluswamy and A.G. Oblad, Preprints, American Chemical Society, Div. Fuel Chem., Anaheim, California, Apr, 1978, Vol. 23, p 107.
5. L. Veluswamy, J. Shabtai and A.G. Oblad, Preprints, American Chemical Society, Div. Fuel Chem., Honolulu, Hawaii, Apr 1979, Vol. 24, p 280.

## Task 7

### Denitrogenation and Deoxygenation of CD Liquids and Related N- and O- Compounds

Faculty Advisor: J. Shabtai  
C. Russell  
Graduate Student: Z. Pai

#### Introduction

The main objective of this research project is to develop effective catalyst systems and processing conditions for reductive hydrodenitrogenation (HDN), as well as for direct (nonreductive) denitrogenation of coal-derived liquids (CDL) in a wide range of nitrogen contents and structural type composition. This is of particular importance in view of the higher concentration of nitrogen-containing compounds in CDL as compared to that of petroleum feedstocks. For a better understanding of denitrogenation processes, the project includes systematic denitrogenation studies not only of CDL but also of related model N-containing compounds found in such liquids, e.g., phenanthridine, 1,10-phenanthroline, carbazoles, acridines, etc., as a function of catalyst type and experimental variables. A part of the study is concerned with determination of the rate, mechanism and stereochemistry of HDN of structurally distinct N-containing aromatic systems in the presence of sulfided catalysts.

#### Project Status

The present report discusses some initial results obtained in a study of the hydrogenation reaction of 1,10-phenanthroline (1) over a sulfided Ni-W/Al<sub>2</sub>O<sub>3</sub> catalyst. Hydrogenation reactions were carried out in an autoclave system described elsewhere.<sup>1</sup> Reaction products were identified by a combination of gas chromatography, mass spectrometry and by comparison with pure reference compounds.

Changes in product composition from hydrogenation of 1 were first investigated as a function of reaction temperature in the range of 200-380°C using a constant pressure of 2500 psig. Initial results obtained are given in Table 1.

As seen from Table 1, the main product from 1 observed at 200°C is 1,2,3,4-tetrahydrophenanthroline (2). With increase in temperature up to 300°C, the yield of 2 gradually decreases while that of 1,2,3,4,7,8,9,10-octahydrophenanthroline (3) gradually increases. The yield of 3 reaches a maximum around 350°C and then decreases at higher temperature. In the 300-380°C range there is gradual formation of (a) partially denitrogenated bicyclic compounds (4), i.e., products in which one of the two nitrogens in the original phenanthroline molecule has been removed; and (b) fully denitrogenated monocyclic compounds (5), e.g., alkylsubstituted benzenes and cyclohexanes. Work on the identification of products of type (a) is presently continuing.

The results obtained indicate that exhaustive denitrogenation of 1 over conventional sulfided Ni-W/Al<sub>2</sub>O<sub>3</sub> catalysts is a slow process occurring to a significant extent only above 350°C. It is further indicated that such catalysts have high ring hydrogenation activity, but rather low C-N (aliphatic) hydrogenolysis activity.

#### Future Work

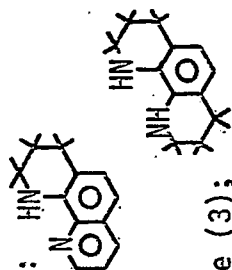
Kinetic rate constants for the hydrogenation-hydrodenitrogenation of 1,10-phenanthroline will be determined in order to clarify the reaction mechanism. The study will involve the use of sulfided Co-Mo and Ni-W catalysts of augmented C-N hydrogenolysis activity (see Task 10).

#### Reference

1. L. Veluswamy, Ph.D. Thesis, University of Utah, Salt Lake City, Utah, 1977.

Table 1. Change in product composition from hydrogenation of 1,10-phenanthroline (1) as a function of temperature.<sup>a</sup>

Reaction Temperature, °C	200	250	300	350	380
Conversion of (1), % by wt	3.7	67.9	100	100	100
Product Components, % by wt:					
1,2,3,4-tetrahydro-phenanthroline (2);	100	94.8	79.1	34.8	20.1
1,2,3,4,7,8,9,10-octahydrophenanthroline (3);	--	0.9	15.5	42.2	6.6
Bicyclic Compounds (4)	--	--	2.2	11.4	32.1
Monocyclic Compounds (5)	--	--	1.7	5.5	23.5



<sup>a</sup>In each experiment were used 10 g of 1 and 1 g of catalyst (sulfided Ni-W/Al<sub>2</sub>O<sub>3</sub>); reaction time, 3 hr; hydrogen pressure, 2500 psi.

## Task 8

### Catalytic Cracking of Hydrogenated Coal-Derived Liquids and Related Compounds

Faculty Advisors: J. Shabtai  
A.G. Oblad  
Graduate Student: S. Sunder

#### Introduction

Hydrogenation followed by catalytic cracking provides a feasible process sequence for conversion of coal liquids into conventional fuels. Such a sequence has certain advantages in comparison with a hydrocracking-catalytic reforming scheme.<sup>1</sup>

The present project is concerned with the following interrelated subjects: (1) systematic catalytic cracking studies of model polycyclic naphthenes and naphthenoaromatics found in hydrogenated coal liquids, e.g., decalin, perhydrophenanthrene, tetralin, 1,2,3,4,5,6,7,8-octahydroanthracene, and 9,10-dihydrophenanthrene, as a function of catalyst type and operating conditions, and (2) systematic catalytic cracking studies of hydrotreated middle-heavy distillate from SRC II as a function of the same variables.

#### Project Status

Results from catalytic cracking studies of model polycyclic naphthenes, e.g., decalin and perhydrophenanthrene, and of model polycyclic naphthenoaromatics, e.g., tetralin, 1,2,3,4,5,6,7,8-octahydroanthracene, 9,10-dihydrophenanthrene, were reported earlier. The results obtained in a systematic catalytic cracking study of hydrotreated solvent refined coal (SRC II) liquids are summarized in this report.

Catalytic cracking of several SRC-II liquid products was investigated as a function of reaction temperature in the range of 375 to 500°C, using the same apparatus and catalyst (Durabead-8) as in the preceding studies of model compounds. The feedstocks used in this part of the study consisted of (A) a middle-heavy distillate fraction of the SRC-II product; and (B) four liquid products obtained by hydrotreatment of the above fraction to different depths. The elemental analyses, C-aromaticities, and densities of these five feedstocks are summarized in Table 1.

Table 2 and Figures 1 and 2 summarize the change in product composition from cracking of hydrotreated SRC-II liquids as a function of reaction temperature. As seen from Table 2 and Figure 1, the yield of C<sub>1</sub>-C<sub>4</sub> gaseous products increases with increasing temperature and with increasing depth of hydrotreatment of the feedstock. Further, it is found that coke formation decreases with increasing temperature and with an increase in the depth of hydrotreatment. Coke formation with the hydrotreated feeds is generally much lower, e.g., 4-9% at 425-500°C, than that found with untreated SRC-II middle-heavy distillate, which yields 19-20% of coke at 425-500°C. A significant improvement in cracking susceptibility is observed when this fraction is hydrotreated even to a small extent prior to catalytic cracking.

As seen from Figure 1, for each hydrotreated liquid studied (IIA, IIB, IIC, and IID), the gasoline yield passes through a maximum, which is at a temperature between 450-475°C for the particular operating conditions (catalyst and LHSV) used. Further, it is found that the gasoline yield increases markedly with increasing depth of hydrotreatment. Up to 66% of the feed can be cracked to gasoline range material (C<sub>5</sub>-230°C).

An increase in cracking susceptibility seems to depend on two factors: heteroatom content and aromaticity. For SRC-IIA and SRC-IIB, the C-aromaticity has been lowered only to a moderate extent, relative to that of untreated SRC-II (see Table 1). On the other hand, heteroatom (O, S, N) contents, especially for SRC-IIB, have been sharply reduced. Apparently, at this mild hydrotreatment stage, the improvement in catalytic cracking is due to (a) major decrease in catalyst poisoning by heteroatom removal; and (b) decrease in the molecular weight and complexity of the feed component by removal of heteroatom linkages between naphthoaromatic clusters. On the other hand, while the heteroatom contents of SRC-IIC and SRC-IID are not very different from each other, a considerable difference in gasoline selectivity (~14% at 450°C) is observed between these two feedstocks, apparently related to the major difference in C-aromaticity (SRC-IIC, 40%; SRC-IID, 12%; see Table 1). Apparently, the improvement associated with deep hydrotreatment (as in SRC-IID) results mostly from hydrogenation of a major portion of the aromatic clusters originally present in the SRC-II middle-heavy distillate.

It can be tentatively concluded that hydrogen added during the early stages of hydrotreatment causes a relatively greater improvement in the catalytic cracking characteristics of coal liquids as compared to the additional improvement resulting from deep hydrotreatment (for hydrogen consumption, see Ref. 1). For example, the H<sub>2</sub> consumed to produce SRC-IIA was only 30% of that consumed to produce SRC-IID. SRC-IIA yields a maximum of 40% gasoline while SRC-IID yields a maximum of 66% gasoline under the operating conditions. While the first improvement in gasoline selectivity of about 37% over SRC-II middle-heavy distillate occurs with 30% of the hydrogen consumed, the further increase of about 26% in gasoline selectivity consumes the remaining 70% of the hydrogen. However, for a final evaluation of optimal hydrotreatment depths, a detailed catalyst deactivation study with hydrotreated SRC-II feeds would be necessary.

Catalytic cracking of one of the hydrotreated SRC liquids (SRC-IIC; C-aromaticity, 40%) was investigated as a function of LHSV (in the range of 3.93 to 0.20 hr<sup>-1</sup>) at 475°C, using the Durabead-8 catalyst. The total process time in each experiment was kept constant at 30 min.

The results obtained are summarized in Table 3 and Figure 3. The product yields show certain similarity to those found in the study of the temperature effect (Table 2, Fig. 1, 2), viz., the yield of gases increases, while the yield of total liquid products slowly decreases with contact time. Further, the yield of gasoline passes through a maximum (55 wt %) around LHSV=0.3 hr<sup>-1</sup>, while coke yield gradually increases with increase in contact time. Also, while coke yield increases with increasing contact time at a given temperature, e.g., 475°C, it decreases with an increase in temperature at a given contact time (Figure 1).

Catalytic cracking of one of the hydrogenated SRC liquids (SRC-IIC, 40% C-aromaticity) was also investigated as a function of reaction temperature (375-500°C) with a Houdry HZ-1 catalyst, for the purpose of a comparison of performance with the Durabead-8 catalyst. The total process time in each experiment was kept constant at 30 min. The product yields are summarized in Table 4, while a comparison between the two catalysts is given in Figure 4. As seen the Houdry HZ-1 catalyst produces more gases and coke than the Durabead-8 catalyst. On the other hand, the latter gives slightly lower yields of gasoline-range liquid products than the HZ-1 catalyst.

#### Reference

1. S. Sunder, Ph.D. Thesis, University of Utah, Salt Lake City, Utah, 1980.

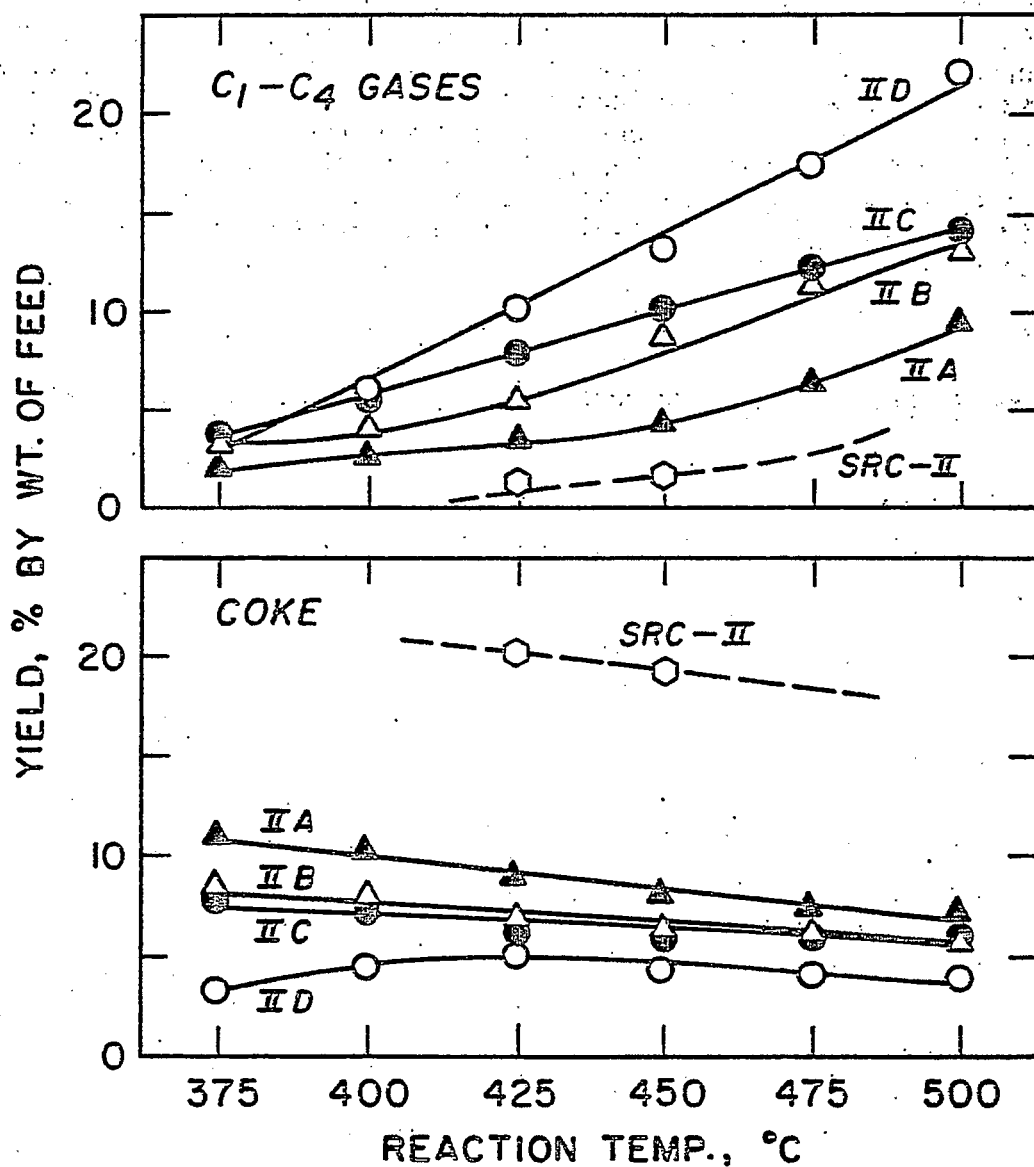


Figure 1. Yield of C<sub>1</sub> - C<sub>4</sub> Gases and Coke from Cracking of Hydrotreated SRC-II Liquids, as a Function of Reaction Temperature and Depth of Hydrotreatment (catalyst, Durabead-8; LHSV, 0.38 hr<sup>-1</sup>; C-aromaticity (%): SRC-II, 64; IIA, 52; IIB, 46; IIC, 40; IID, 12).

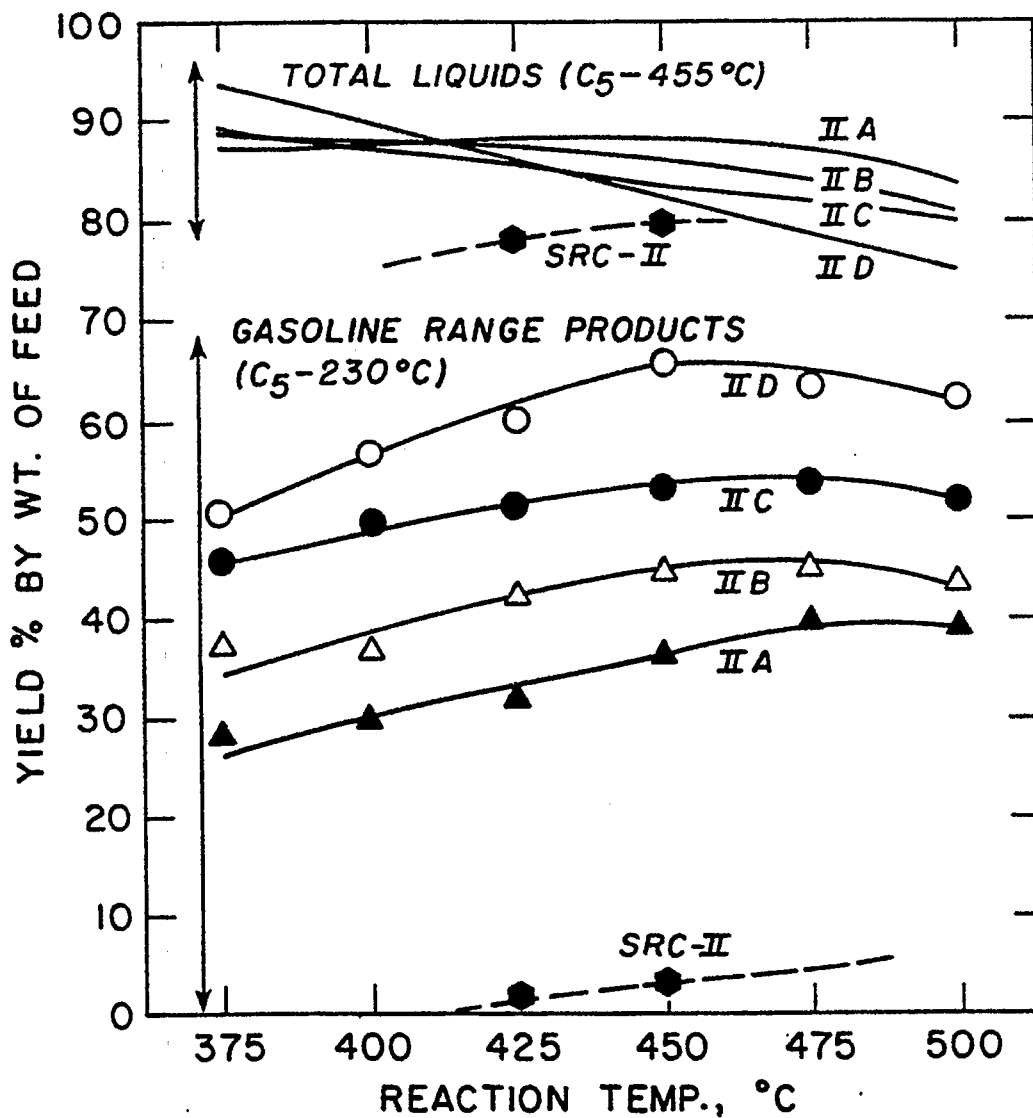


Figure 2. Total Liquids Yield and Gasoline Liquids (C<sub>5</sub> - 230°C) Yield from Cracking of Hydrotreated SRC-II as a Function of Reaction Temperature and Depth of Hydrotreatment (catalyst, Durabead-8; LHSV, 0.38 hr<sup>-1</sup>; C-aromaticity (%): SRC-II, 64; IIA, 52; IIB, 46; IIC, 40; IID, 12).

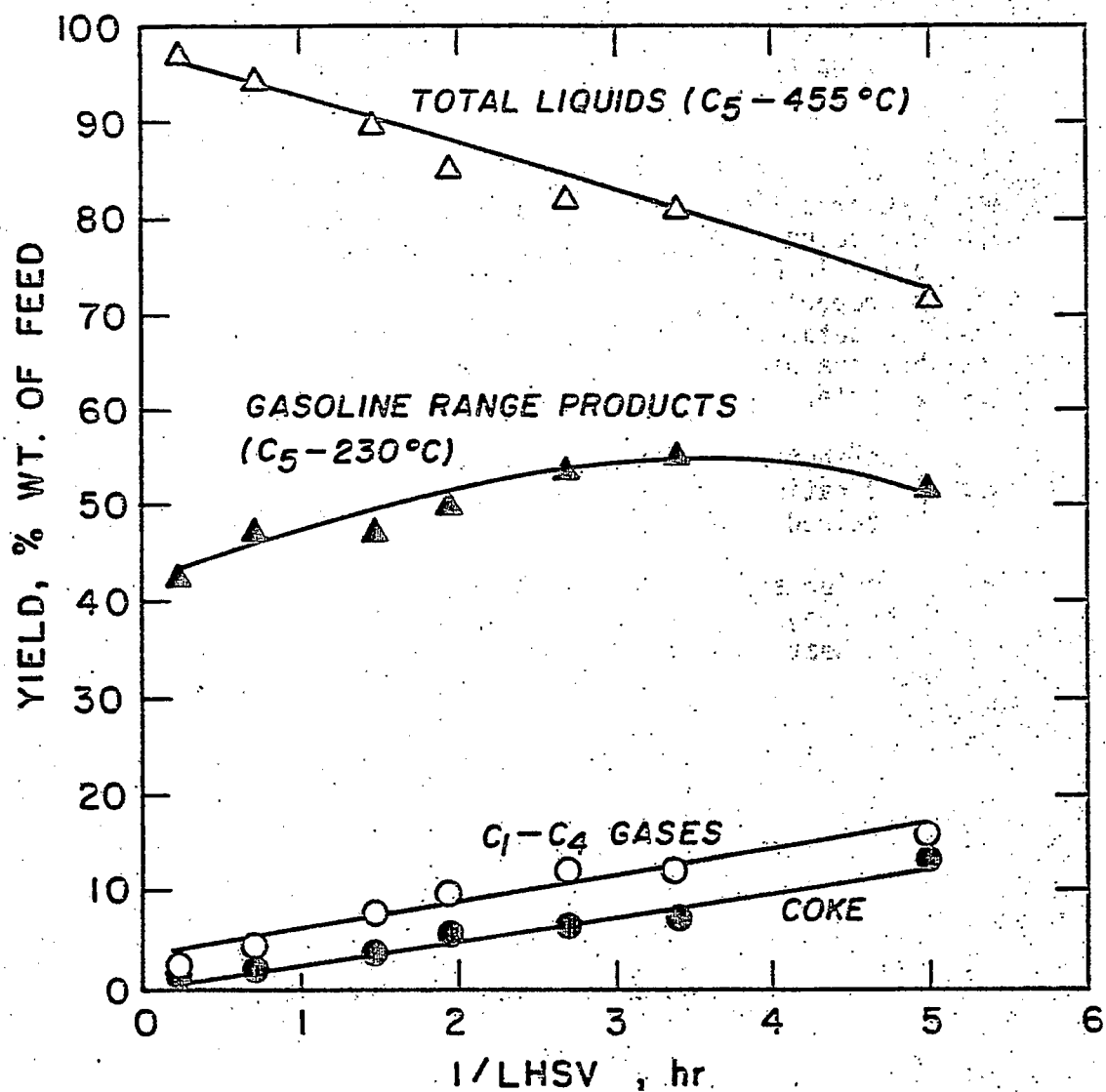


Figure 3. Change in Product Composition from Cracking of Hydrotreated SRC-II. (40% Aromatic Carbon) as a Function of LHSV (catalyst, Durabead-8; reaction temperature, 475°C).

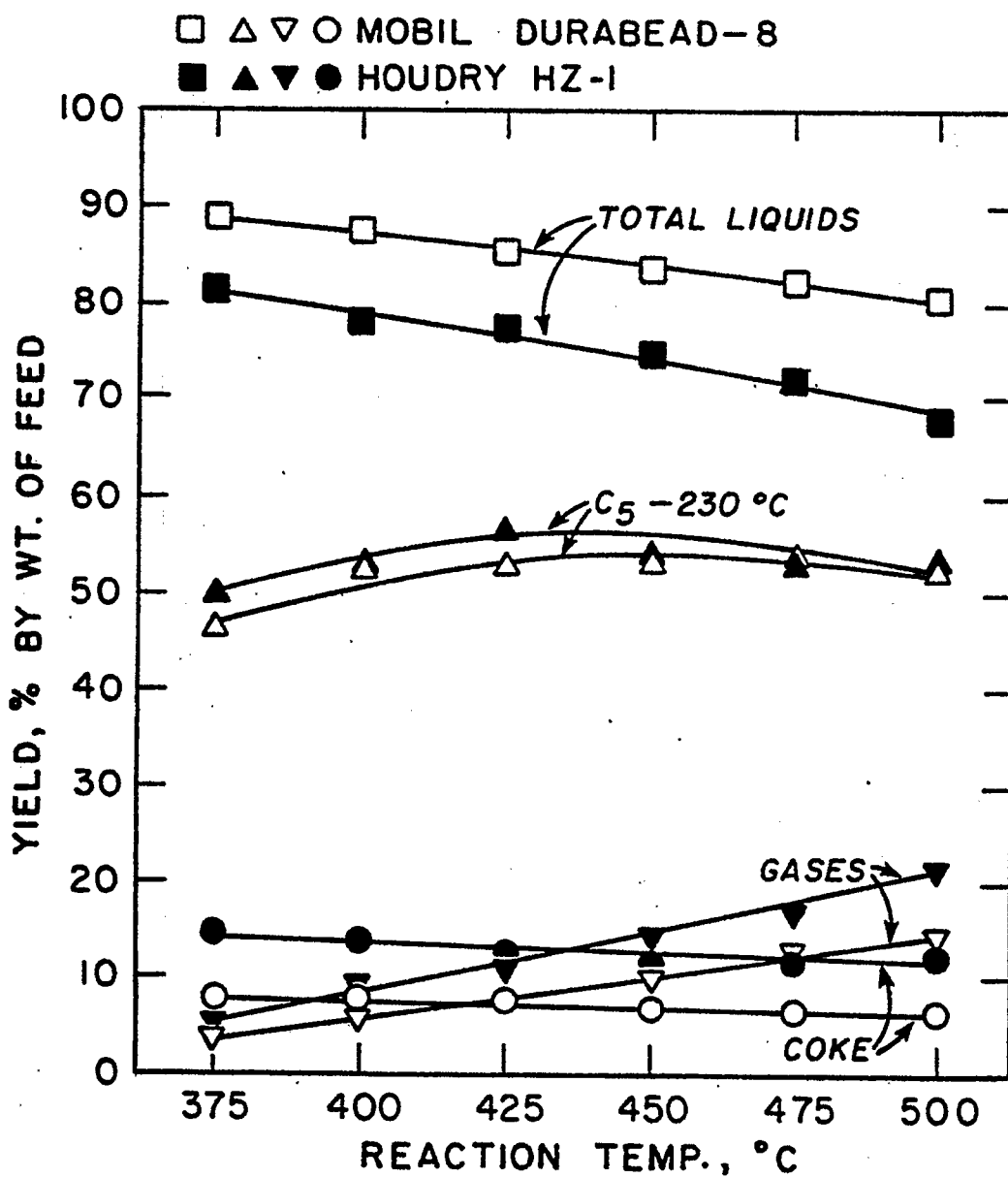


Figure 4 . Change in Product Composition from Cracking of Hydrotreated SRC-II (40% Aromatic Carbon) as a Function of Reaction Temperature and Catalyst Type (LHSV, 0.38 hr<sup>-1</sup>).

Table 1

## Properties of Untreated and Hydrotreated SRC-II Liquid Feedstocks.

Type of feedstock	Untreated middle-heavy distillate fr. <sup>a</sup>	Hydrotreated SRC-II liquids <sup>b,c</sup>				
		SRC-II	SRC-IIA	SRC-IIB	SRC-IIC	SRC-IID
Denotation						
Elemental Composition, % by wt.						
Carbon	87.29	87.90	88.32	88.03	86.35	
Hydrogen	8.34	10.00	10.60	11.45	13.54	
Oxygen	2.90	1.00	0.80	< 0.5	< 0.1	
Nitrogen	1.20	1.09	0.28	< 0.014	< 0.01	
Sulfur	0.27	< 0.01	< 0.01	0	0	
C-Aromaticity, %	64	52	46	40	12	
Density, g/cc	1.28	1.16	1.15	1.15	1.01	

<sup>a</sup>B. p. range, 230 - 455°C; <sup>b</sup>Obtained by hydrotreatment of SRC-II middle-heavy distillate fraction (hydrogenation depth increases gradually from SRC-IIA to SRC-IID); <sup>c</sup>For hydrotreatment conditions see Reference 1.

Table 2

Change in Product Composition from Cracking of Hydrotreated SRC-II  
Liquids as a Function of Reaction Temperature<sup>a-d</sup>.

Reaction Temperature, °C	375	400	425	450	475	500
Feedstock: Untreated SRC-II <sup>e</sup>						
Experiment Number			SRC 139	SRC 124		
Conversion <sup>f</sup>	-	-	2.5	4.3	-	-
Product Distribution, wt. % of feed						
(a) C <sub>1</sub> - C <sub>4</sub> gases	-	-	1.0	1.3	-	-
(b) Total Liquids (C <sub>5</sub> - 455°C)	-	-	79.0	79.8	-	-
(c) Coke	-	-	20.0	18.9	-	-
Gasoline-range fraction (C <sub>5</sub> - 230°C)	-	-	1.5	3.0	-	-

Table 2 - Continued

Reaction Temperature, °C	375	400	425	450	475	500
Feedstock: SRC-IIA9						
Experiment Number	SRC 138	SRC 137	SRC 136	SRC 134	SRC 133	SRC 135
Conversion <sup>f</sup>	30.0	32.7	35.1	40.3	45.9	48.3
Product Distribution, wt. % of feed						
(a) C <sub>1</sub> - C <sub>4</sub> gases	1.9	2.6	3.3	4.1	6.3	9.3
(b) Total liquids (C <sub>5</sub> - 455°C)	87.1	87.3	88.0	88.2	86.2	83.7
(c) Coke	11.0	10.1	8.8	7.7	7.5	6.9
Gasoline-range fraction (C <sub>5</sub> - 230°C)	28.1	30.1	31.8	36.2	39.6	39.0

Table 2 - Continued

Reaction Temperature, °C	375	400	425	450	475	500
Feedstock: SRC-IIB <sup>h</sup>						
Experiment Number	SRC 132	SRC 131	SRC 130	SRC 128	SRC 127	SRC 129
Conversion <sup>f</sup>	40.2	40.2	47.3	53.1	56.2	56.2
Product Distribution, wt. % of feed						
(a) C <sub>1</sub> - C <sub>4</sub> gases	2.9	3.9	5.3	8.5	11.2	12.9
(b) Total liquids (C <sub>5</sub> - 455°C)	88.6	88.0	87.7	85.3	82.7	81.1
(c) Coke	8.5	8.1	7.0	6.2	6.2	5.9
Gasoline-range fraction (C <sub>5</sub> - 230°C)	37.3	36.3	42.0	44.6	45.0	43.3

Table 2 - Continued

Reaction Temperature, °C	375	400	425	450	475	500
Feedstock: SRC-IIC <sup>1</sup>						
Experiment Number	SRC 108	SRC 107	SRC 111	SRC 106	SRC 109	SRC 110
Conversion <sup>f</sup>	49.5	54.8	58.9	62.9	65.5	65.9
Product Distribution, wt. % of feed						
(a) C <sub>1</sub> - C <sub>4</sub> gases	3.5	5.4	7.7	10.0	12.0	14.0
(b) Total Liquids (C <sub>5</sub> - 455°C)	88.7	87.2	87.8	83.3	81.9	80.0
(c) Coke	7.8	7.4	6.2	6.8	6.1	6.0
Gasoline-range fraction (C <sub>5</sub> - 230°C)	46.0	49.4	51.2	52.9	53.5	51.9

Table 2 - Continued

Reaction Temperature, °C	375	400	425	450	475	500
Feedstock: SRC-IID <sup>j</sup>						
Experiment Number	SRC 102	SRC 105	SRC 103	SRC 104	SRC 125	SRC 126
Conversion <sup>f</sup>	53.5	62.4	66.9	78.5	80.8	84.1
Product Distribution, wt. % of feed						
(a) C <sub>1</sub> - C <sub>4</sub> gases	3.1	5.7	9.9	12.9	17.4	21.9
(b) Total liquids (C <sub>5</sub> - 455°C)	93.8	89.9	85.2	83.0	78.6	74.3
(c) Coke	3.1	4.4	4.9	4.1	4.0	3.8
Gasoline-range fraction (C <sub>5</sub> - 230°C)	50.4	56.7	57.0	65.6	63.4	62.2

<sup>a</sup>In each experiment 4.6 cc of feed was used;

<sup>b</sup>Catalyst, Durabead-8, 20 g;

<sup>c</sup>Run time, 30 min.;

<sup>d</sup>LHSV, 0.38 hr<sup>-1</sup>;

<sup>e</sup>C-Aromaticity (%), 64;

<sup>f</sup>Conversion into gaseous and liquid products boiling < 230°C;

<sup>g</sup>C-Aromaticity (%), 52;

<sup>h</sup>C-Aromaticity (%), 46;

<sup>i</sup>C-Aromaticity (%), 40;

<sup>j</sup>C-Aromaticity (%), 12.

Table 3

Change in Product Composition from Cracking of SRC-IIC  
as a Function of LHSV<sup>a-e</sup>.

Experiment Number	SRC 114	SRC 113	SRC 112	SRC 115	SRC 109	SRC 116	SRC 123
LHSV, hr <sup>-1</sup> (1/LHSV)	3.93 (0.25)	1.42 (0.70)	0.68 (1.47)	0.51 (1.96)	0.38 (2.63)	0.30 (3.33)	0.20 (5.00)
Conversion (into gaseous + liquid products < 230°C)	44.3	51.1	54.3	59.7	65.5	66.6	67.2
Product Distribution, wt. % of feed							
(a) C <sub>1</sub> - C <sub>4</sub> gases	2.1	4.0	7.3	9.8	12.0	11.8	15.5
(b) Total liquids (C <sub>5</sub> - 455°C)	96.8	94.2	89.4	85.1	81.9	81.1	71.3
(c) Coke	1.1	1.8	3.3	5.2	6.1	7.0	13.2
Gasoline-range fraction (C <sub>5</sub> - 230°C)	42.2	47.1	47.0	49.9	53.5	54.8	51.7

<sup>a</sup>In each experiment 4.6 cc of feed was used; <sup>b</sup>Catalyst, Durabead-8; <sup>c</sup>Run time, 30 min.; <sup>d</sup>Reaction temperature, 475°C; <sup>e</sup>for properties of SRC-IIC, see Table 1.

Table 4

Change in Product Composition from Cracking of SRC-IIC as a Function of Reaction Temperature (Catalyst, Houdry HZ-1)<sup>a-e</sup>.

Experiment Number	SRC 119	SRC 117	SRC 118	SRC 120	SRC 121	SRC 122
Reaction Temperature, °C	375	400	425	450	475	500
Conversion (into gaseous + liquid products < 230°C)	54.0	60.9	67.0	67.9	69.3	73.6
Product Distribution, wt. % of feed						
(a) C <sub>1</sub> - C <sub>4</sub> gases	4.4	8.7	10.7	14.1	16.5	21.0
(b) Total liquids (C <sub>5</sub> - 455°C)	81.2	77.8	77.1	74.5	71.8	67.6
(c) Coke	14.4	13.4	12.2	11.4	11.2	11.5
Gasoline range fraction (C <sub>5</sub> - 230°C)	49.6	52.2	56.3	53.8	52.8	52.6

<sup>a</sup>In each experiment 4.6 cc of feed was used; <sup>b</sup>Catalyst, Houdry HZ-1, 20 g; <sup>c</sup>Run time, 30 min.;

<sup>d</sup>LHSV, 0.38 hr<sup>-1</sup>; <sup>e</sup>for properties of SRC-IIC, see Table 1.

Systematic Structural Activity Study of Supported  
Sulfide Catalysts for Coal Liquids Upgrading

Faculty Advisors: F.E. Massoth  
J. Shabtai  
Post-Doctoral Fellow: G. Muralidhar

Introduction

The objective of this research is to develop an insight into basic properties of supported sulfide catalysts and to determine how these relate to coal liquids upgrading. The proposed program involves a fundamental study of the relationship between the surface-structural properties of various supported sulfide catalysts and their catalytic activities for various types of reactions. Thus, there are two clearly defined and closely related areas of investigation, viz., (1) catalyst characterization, especially of the sulfided and reaction states and (2) elucidation of the mode of interaction between catalyst surfaces and organic substrates of different types. The study of subject (1) will provide basic data on sulfided catalyst structure and functionality, and would allow the development of catalyst surface models. Subject (2), on the other hand, involves systematic studies of model reactions on sulfide catalysts, and the utilization of data obtained for development of molecular level surface reaction models correlating the geometry (and topography) of catalyst surfaces with the steric-conformational structure of adsorbed organic reactants. The overall objective of the project is to provide fundamental data needed for design of specific and more effective catalysts for upgrading of coal liquids.

Atmospheric activity tests using model compounds representative of hydrodesulfurization (thiophene), hydrogenation (hexene) and cracking (isooctene) have been developed. These were employed to assay changes in the catalytic functions of various supported CoMo catalysts. It was found that hydrodesulfurization (HDS) and hydrogenation activities were generally unaffected by the type of alumina used or by the cobalt salt used in the preparation; whereas, cracking activity varied considerably, being highest for  $\gamma$ -Al<sub>2</sub>O<sub>3</sub> and cobalt sulfate addition. In a series of catalysts employing silica-alumina as the support, the two former functions decreased with increasing silica content, while cracking went through a maximum in activity.

Project Status

During this period, the effects of adding an acidic and a basic promoter to the standard CoMo/Al<sub>2</sub>O<sub>3</sub> catalyst were evaluated. Also, a step-wise addition of cobalt was prepared and tested.

The general method of catalyst preparation was described in the previous report. The standard catalyst consisted of 3% Co and 8% Mo supported on  $\gamma$ -Al<sub>2</sub>O<sub>3</sub>. The additives were incorporated at 0.5 wt % levels by an incipient wetness technique, using a solution of sodium nitrate or ammonium fluoride. Addition

was performed in two modes: (1) to the calcined support or (2) to the finished calcined catalyst. In the first case, the altered support was recalcined prior to addition of cobalt and molybdenum. A special catalyst was prepared by step-wise impregnation of the cobalt instead of the normal single impregnation. This consisted of three additions of 1% Co to the 8% Mo/Al<sub>2</sub>O<sub>3</sub> catalyst, with calcination at 540°C between additions. In all cases, the final catalyst was oven-dried and then calcined overnight at 540°C. The calcined catalysts were sulfided and tested for hydrodesulfurization, hydrogenation and cracking activities using thiophene, hexene-1 and isooctene as model reactions. Details of the experimental procedure were given previously.<sup>1</sup>

The results of the activity tests are given in Table 1, in terms of rate constants for the indicated reactions. Significant differences in HDS and cracking activities were observed between the various catalysts, whereas hydrogenation activities were not greatly different. For the additives, the mode of addition, either to the support first or to the finished catalyst, had little effect on the resultant activities. This is somewhat surprising, as the presence of the additive on the support was expected to affect the subsequent disposition of the Co and Mo phases in the final calcined catalyst; whereas its addition to the calcined catalyst should not affect the Co and Mo phases, which are already set in the catalyst. Possibly, the subsequent sulfiding minimized any such effects that may have been present in the calcined catalyst.

The HDS activities for the catalysts with added fluoride was about the same as for the standard CoMo/Al<sub>2</sub>O<sub>3</sub> catalyst. Addition of fluoride to Al<sub>2</sub>O<sub>3</sub> is known to increase the acidity of the Al<sub>2</sub>O<sub>3</sub>, and this was observed in the increased cracking activities of these catalysts as compared with the standard catalyst. That this increased acidity had little effect on the HDS activity is contrary to results obtained previously using silica-alumina as the supports, the latter catalysts showing a marked decrease in HDS activity.<sup>1</sup> It has been tentatively concluded that the lower HDS activity for the silica-alumina supported catalysts must be due to a support effect, giving a less effective active phase area, than to an acidity effect. This conclusion is further supported by the lower hydrogenation activities also observed with the silica-alumina supported catalysts, in contrast to no loss in hydrogenation activity for the fluoride-promoted catalyst.

The addition of sodium resulted in a lowering in both HDS and cracking activity. Since sodium will cause a decrease in acidity of the catalyst, the lower cracking activity of these catalysts is understandable on the basis that cracking is strongly related to the catalyst acidity. This was observed in the silica-alumina series run previously. The effect of sodium on HDS activity is less clear. As sodium oxide, it may adsorb on some sulfur anion vacancies in the MoS<sub>2</sub> phase, which are believed to be the active sites for HDS,<sup>2</sup> thus reducing their number. At any rate, the hydrogenation activity was not affected by sodium. Hydrogenation appears to be the least sensitive function to be affected by additives.

Addition of cobalt by step-wise impregnation gave a remarkable increase in HDS activity over that of the standard single step impregnation. This is in agreement with some earlier work on this mode of preparation.<sup>3</sup> However, hydrogenation and cracking functions were much less affected in this catalyst.

In developing viable processes for upgrading coal liquids, a distinct disadvantage is excessive hydrogen consumption. For selective heteroatom sulfur removal, a high ratio of HDS to hydrogenation would be advantageous. If the results of the low pressure, model compound tests adopted here, showing relative catalytic functions, were to approximately apply to realistic processing conditions, then catalysts having relatively high  $k_T/k_H$  ratios should perform best for heteroatom sulfur removal. Neither the addition of a strong acidic component (fluoride) nor basic component (sodium) improved this ratio over the standard catalyst. The step-addition of Co, however, increased the  $k_T/k_H$  ratio by 60%, and might be considered a superior catalyst for this purpose.

In treating coal liquids, another important catalytic function is cracking, in order to break down the larger molecular weight fractions to products in the gasoline range. Again, excessive hydrogenation is undesirable. Therefore, catalysts having high relative cracking to hydrogenation functions are desirable. Here, higher acidity is believed to be important. The addition of fluoride showed an improved  $k_C/k_H$  ratio, whereas addition of sodium gave a lower  $k_C/k_H$  ratio. The Co-step catalyst also gave a higher  $k_C/k_H$  ratio, which would seem to indicate that the disposition of the cobalt somehow affects catalyst acidity.

#### Future Work

Work will continue on the effect of different supports and additives on catalyst properties and activities. Supports to be tested include  $TiO_2$ ,  $SiO_2-MgO$ ,  $ZrO_2$  and a pure  $Al_2O_3$ . Additional additives planned for evaluation are Cl, P, Mg, Ca, Ti and Zr.

#### References

1. W.H. Wiser, F.E. Massoth and J. Shabtai, DOE Contract No. DE-AC01-79ET14700, Quarterly Progress Report, Salt Lake City, Utah, Jan-Mar 1980.
2. F.E. Massoth, Adv. Catal., 27, 265 (1978).
3. C.K. Chung, Ph.D. Thesis, University of Utah, Salt Lake City, Utah, 1979.

Table 1. Effect of additives on activity of CoMo/Al<sub>2</sub>O<sub>3</sub> catalysts.

Catalyst <sup>a</sup>	$k_T^b$ cm <sup>3</sup> /g min atm	$k_H^b$ cm <sup>3</sup> /g min	$k_C^b$ cm <sup>3</sup> /g min	$k_T/k_H$	$k_C/k_H$
CoMo/Al <sub>2</sub> O <sub>3</sub> <sup>c</sup>	33.6	63.7	150	0.53	2.35
CoMo/Al <sub>2</sub> O <sub>3</sub> + F	39.7	72.9	215	0.54	2.95
CoMoF/Al <sub>2</sub> O <sub>3</sub>	35.6	71.8	222	0.50	3.09
CoMo/Al <sub>2</sub> O <sub>3</sub> + Na	25.0	61.2	101	0.41	1.65
CoMoNa/Al <sub>2</sub> O <sub>3</sub>	19.6	61.8	104	0.32	1.68
Co(s)Mo/Al <sub>2</sub> O <sub>3</sub> <sup>d</sup>	60.6	70.2	210	0.86	2.99

<sup>a</sup>All catalysts contain 3% Co and 8% Mo on  $\gamma$ -Al<sub>2</sub>O<sub>3</sub>. Additives at 0.5% level.

<sup>b</sup>Rate constants are  $k_T$  for HDS,  $k_H$  for hydrogenation,  $k_C$  for cracking.

<sup>c</sup>Standard catalyst for comparison purposes.

<sup>d</sup>Co added in 1% step.

## Task 12

### Diffusion of Polyaromatic Compounds in Amorphous Catalysts Supports

Faculty Advisor: F.E. Massoth  
Graduate Student: A. Chantong

#### Introduction

This project involves assessing diffusional resistances within amorphous-type catalysts. Of primary concern is the question of whether the larger, multiring hydro-aromatics found in coal-derived liquids will have adequate accessibility to the active sites within the pores of typical processing catalysts. When molecular dimensions approach pore size diameters, the effectiveness of a particular catalyst is reduced owing to significant mass transport resistance. An extreme case occurs when molecular and pore sizes are equivalent, and pores below this size are physically inaccessible.

The project objective can be achieved through a systematic study of the effect of molecular size on sorptive diffusion rates relative to pore geometry. Conceptually, the diffusion of model aromatic compounds is carried out using a stirred batch reactor. The preferential uptake of the aromatic from the aliphatic solvent is measured using a UV spectrometer. Adsorption isotherms are determined to supplement the diffusion studies.

Initial work entailed development of a suitable reactor, measurement techniques and methods of data analysis. These demonstrated that adsorption was diffusion-controlled. Effective diffusivities were larger than predicted for pore diffusion and a surface diffusion contribution was postulated. Subsequent studies were extended to other multiaromatic compounds and aluminas with similar results. The fractional surface diffusion contribution was appreciable and about the same in all cases. Because of this, restrictive diffusion effects could not be properly evaluated. However, for the largest size compound (20Å) and smallest average pore size alumina (50Å) tested, a markedly lower diffusivity was obtained, indicative of a restrictive diffusion effect.

#### Project Status

It had been shown in the last report<sup>1</sup> that equilibrium adsorption of naphthalene in cyclohexane with catalyst D was nonlinear and a Freundlich isotherm was used in fitting the data. If the equilibrium adsorption is not linear, the curvature of the equilibrium adsorption curve has to be taken into account in calculating an effective diffusivity from kinetic runs. Therefore, the equilibrium adsorption is needed to properly evaluate the diffusion runs.

Equilibrium adsorptions of coronene and meso-tetraphenylprophine are shown in Figure 1. Both curves are fitted by Freundlich isotherm, which is represented by the following equation:

$$M_f = kc_f^{1/n}$$

where  $M_f$  is the final solute uptake in mg/cc catalyst,  $C_f$  is the final solute concentration in mg/l, and  $k$  and  $n$  are constants for a given solute and catalyst.

Table 1 shows the values of  $k$  and  $n$  for naphthalene, coronene, and meso-tetraphenylporphine with catalyst D. The values of  $k$  and  $n$  for naphthalene are taken from the last report. The catalysts were calcined at 500°C for each experiment. Table 1 illustrates that the higher the molecular weight of the aromatic compound, the higher are the values of  $k$  and  $n$ . For a higher value of  $n$ , the solute will be adsorbed stronger and the curvature of equilibrium adsorption curve will be more pronounced.

#### Future Work

Kinetic runs for coronene and meso-tetraphenylporphine with catalyst D will be carried out.

#### Reference

1. W.H. Wiser, F.E. Massoth and A. Chantong, DOE Contract No. DE-AC01-79ET14700, Quarterly Progress Report, Salt Lake City, Utah, Apr-June 1980.

TABLE 1

Values of  $k$  and  $n$  for the aromatic compounds with catalyst D.

<u>Solutes</u>	<u>Molecular Weight</u>	<u>k</u>	<u>n</u>
Naphthalene	128	15.4	1.26
Coronene	300	128.4	1.50
Meso-tetraphenylporphine	614.8	172.2	1.95

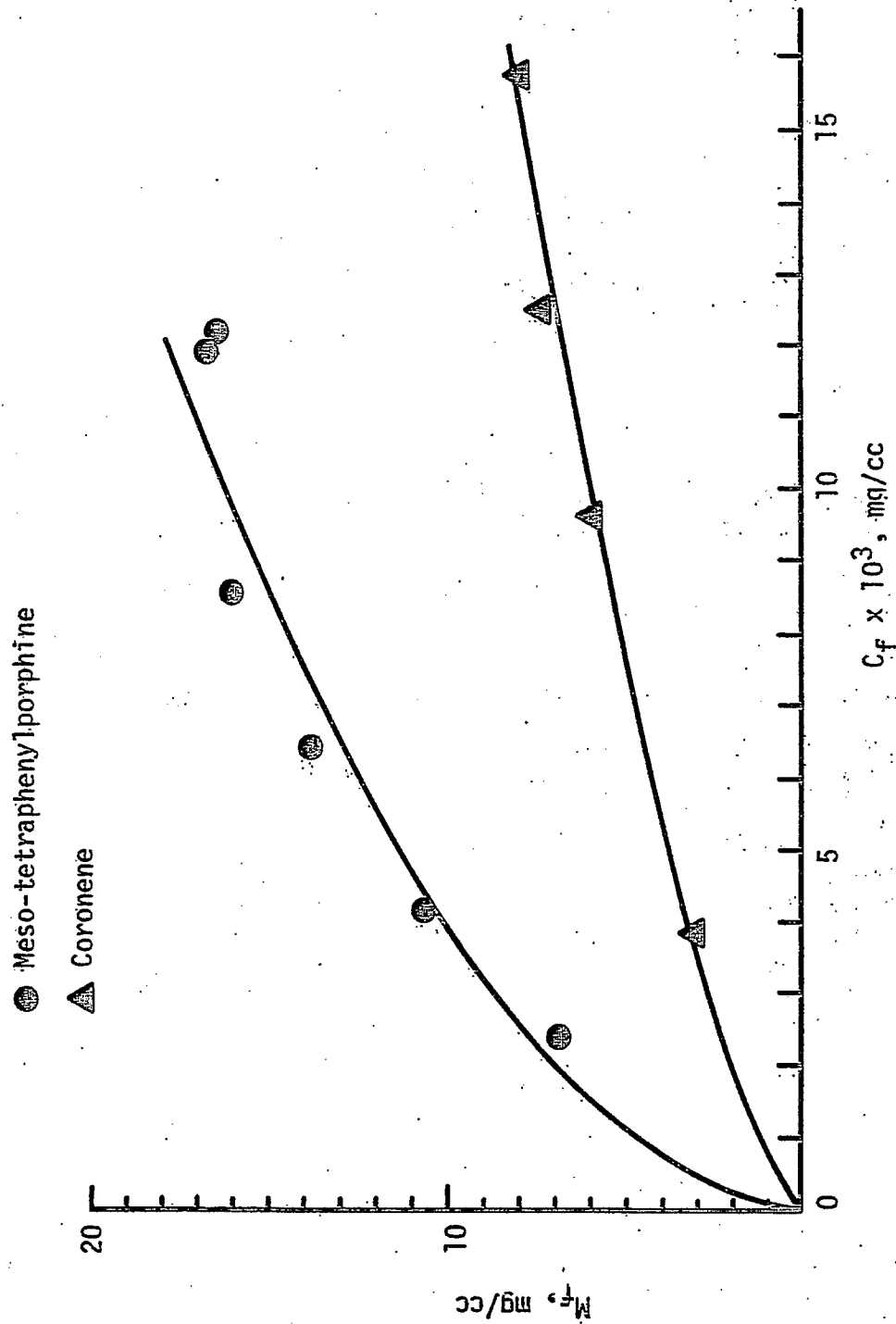


Figure 1. Isothermal adsorptions of aromatic compounds in cyclohexane with catalyst D.

## Task 13

### Catalyst Research and Development

#### Synthesis of Light Hydrocarbons from CO and H<sub>2</sub>

Faculty Advisor: F.V. Hanson

Graduate Student: Y.S. Tsai

#### Introduction

The hydrogenation of carbon monoxide for the production of low molecular weight olefins (C<sub>2</sub>-C<sub>4</sub>) has been investigated over a variety of metallic catalysts. In particular, iron-manganese catalysts have exhibited significant selectivity for low molecular weight olefins. The data of catalyst screening tests indicated that an iron-manganese catalyst composed of 2.2 parts manganese per 100 parts iron (atomic ratio) was selective for the production of C<sub>2</sub>-C<sub>4</sub> olefins. Effects of process variables on the product yield and selectivity over a subset of the iron-manganese have been completed. Most of the data agreed with that found in the literature.

To obtain a more comprehensive analysis of the catalyst performance, the following steps will be taken:

- (1) The modification of the fixed-bed reactor system.
- (2) The establishment of the catalyst characterization procedures to determine relationships between the catalyst activity and selectivity and the nature of the catalyst surface.
- (3) The effects of various catalyst pretreatments and catalyst preparation on the yield and the selectivity.

#### Project Status

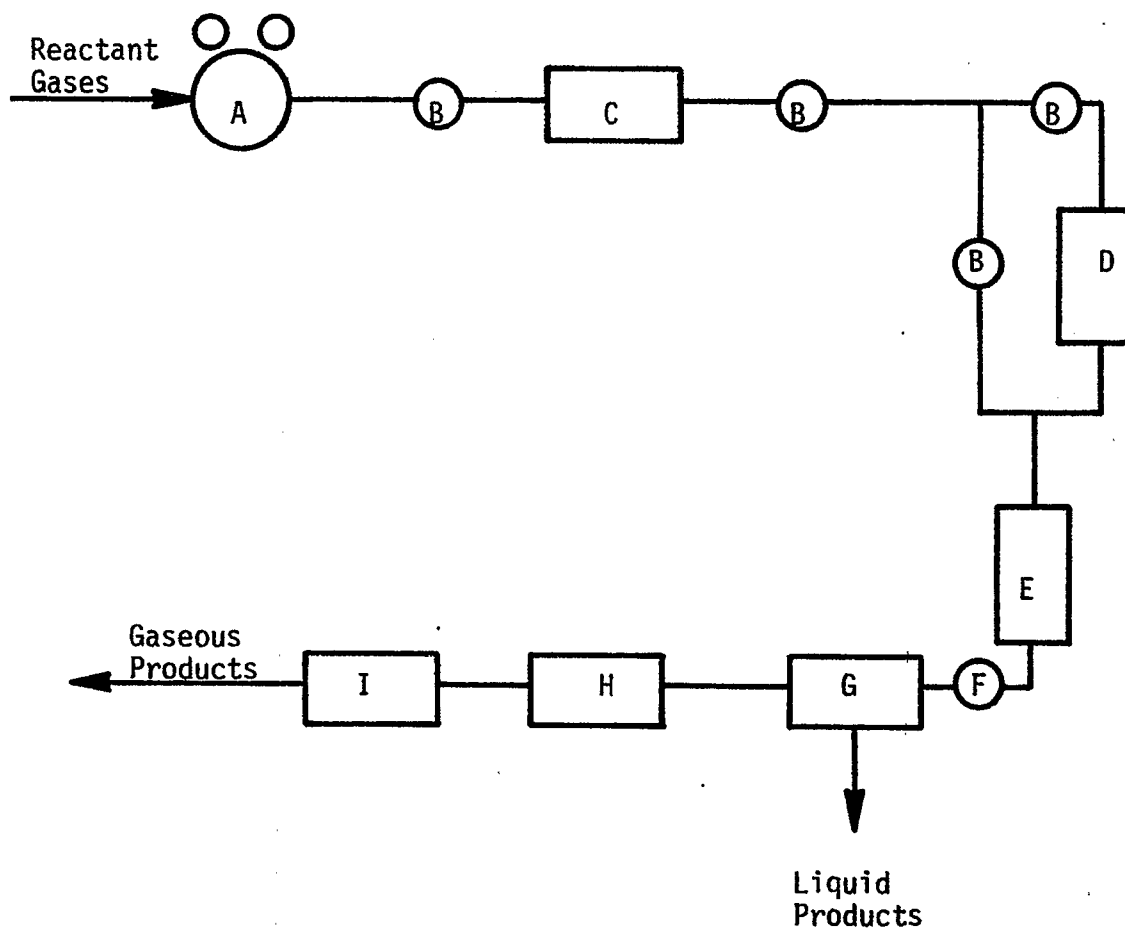
The new fixed-bed reactor system is being designed. A schematic of the system is shown in Figure 1. The synthesis gas first passes through the activated carbon purifier for the removal of trace metal carbonyls. The input flowrate of the mixture will be measured by a rotameter. The synthesis of hydrocarbons will be carried out in a vertical fixed-bed reactor to minimize the possible entrainment of high molecular weight hydrocarbons from the reaction in the reactor. The product gas and vapor from the reactor will pass through the liquid product trap and cold trap to condense the high boiling point hydrocarbons and water in the product gases. The output flowrate of gaseous products will be measured by a wet-test meter. The compositions of the gases will be analyzed by a gas chromatograph. In the system a metering valve connected below the reactor will serve to control the flowrate of the synthesis gas and to reduce the gas pressure to the atmospheric pressure.

Some equipment has been purchased. The procedures for catalyst characterization and also catalyst testing are being done simultaneously.

### Future Work

The fabrication of the system will be carried out after the equipment is acquired. Some iron-manganese catalysts will be tested by characterization techniques. A literature survey will also be initiated.

Figure 1. A schematic of the fixed-bed reactor system.



A-In-line Pressure Regulator  
B-Control Valve  
C-Activated Carbon Purifier  
D-Rotameter  
E-Fixed-Bed Reactor

F-Metering Valve  
G-Liquid Hydrocarbon Trap  
H-Cold Trap  
I-Wet-Test Meter

## Task 13

### Catalyst Research and Development

Faculty Advisor: F.V. Hanson  
Graduate Student: C.S. Kim

#### Introduction

The objectives of this project are to develop a preparation technique for a Raney type catalyst (particularly Raney iron-manganese catalyst) and to find the optimum process variables for the maximum production of low molecular weight olefins and/or BTX via hydrogenation of carbon monoxide. A detailed description of the objectives are in a previous report.<sup>1</sup>

A fixed-bed reactor system was fabricated to conduct catalyst screening tests to determine the optimum process variables, and to study the overall kinetics of the hydrogenation of carbon monoxide over Raney type catalyst. A detailed flow diagram has been already presented.<sup>2</sup>

An electrically heated furnace was designed to produce Al-Fe-Mn alloys with various compositions. These alloys will be used as a starting material in the synthesis of Raney type catalysts. A detailed flow diagram of the furnace is found in a previous report.<sup>3</sup>

#### Project Status

The construction work for the furnace has been completed and it is ready to use at the present time. Due to the unavailability of a proper power source for the furnace in this lab, the production of Raney alloys could not be initiated. In a few weeks the furnace will be located in a new building, in which a proper power source is available.

#### Future Work

As soon as the power source is available, various alloy samples with different compositions will be made. These alloys will be subjected to size reduction and activation with a caustic solution. Various parameters in the activation procedure, such as particle size, caustic solution concentration, digestion temperature, and digestion time, will be studied in detail in connection with the catalyst activity and selectivity tests in the fixed-bed reactor.

#### References

1. W.H. Wiser, F.V. Hanson and C.S. Kim, DOE Contract No. DE-AC01-79ET14700, Quarterly Progress Report, Salt Lake City, Utah, Oct-Dec 1979.
2. ibid., Jan-Mar 1980.
3. ibid., April-June 1980.

## Task 14

### Characterization of Catalysts and Mechanistic Studies

Faculty Advisor: F.E. Massoth  
Graduate Student: K.B. Jensen

#### Introduction

This phase of the project is intended to supplement the high pressure reactor studies by detailed examination of the catalyst properties which enhance catalyst activity and selectivity. This is accomplished by characterization studies performed on fresh catalysts and on the same catalysts which have been run in the reactor. Of particular interest are metal areas, phase structure, catalyst stability and surface characteristics. Also, variables in catalyst preparation and pretreatment are examined to establish their effects on catalyst properties. Finally, in-situ adsorption and activity are studied under modified reaction conditions with a number of well-characterized catalysts to obtain correlating relationships. The catalysts under present investigation are iron-based catalysts promoted with manganese oxide.

Previous work had shown the reduced catalysts have low surface areas ( $<10 \text{ m}^2/\text{g}$ ) and are composed of two principal phases,  $\alpha$  iron and manganese (II) oxide. Some used catalysts were also found to contain small amounts of possible iron oxide and iron carbide phases. Investigations using the scanning electron microscope indicated that the MnO phase is well dispersed in the catalysts and X-ray line broadening results indicated that the MnO particles or possible layers average in the order of 200 Å in breadth. Some iron (II) oxide (FeO) is also indicated to be present in the MnO phase by X-ray diffraction.

Preliminary carburization studies gave two general regimes of carburization, an early fast carburization followed by a slower one. The presence of MnO promoter was found to slow carburization.

#### Project Status

Temperature programmed desorption/reaction (TPD/TPR) studies were continued. All catalysts were reduced initially in hydrogen at 500°C overnight and then purged with helium at the same temperature for about a half hour and then cooled to room temperature. The catalysts were exposed to adsorbate gas at room temperature for a half hour, flushed in He or N<sub>2</sub> for approximately 10 min, and then heated in a programmed schedule (8-10°C/min) to 500°C in flowing He or H<sub>2</sub>. The off gases were monitored by a mass spectrometer. The flow rates usually varied between 30-40 cc/min, and all experiments were performed at atmospheric pressure. The presence of 0.77% argon in the helium provided a marker peak in the mass spectra when this carrier gas was used.

The following sequence was employed in the TPD/TPR studies after initial reduction: Step (1) CO was passed over the catalyst for ½ hour, then it was

flushed with He and temperature programmed in He to 500°C (TPD) and afterwards cooled. Step (2) At room temperature the reactor gas was changed to H<sub>2</sub> and then the catalyst was temperature programmed in H<sub>2</sub> (TPR) so that H<sub>2</sub> could react with any carbonaceous species or surface oxygen left on the catalyst after Step (1). Step (3) After cooling in H<sub>2</sub> again to room temperature, the catalyst was exposed to CO for ½ hour. The catalyst was briefly flushed with H<sub>2</sub> and then temperature programmed in H<sub>2</sub>. Step (4) The catalyst was cooled to 250°C and synthesis gas (H<sub>2</sub>/CO=2.0) was used to carburize the catalyst for 2 hours at this temperature. The catalyst was then cooled to room temperature in synthesis gas and then CO was passed over the catalyst for ½ hour. The catalyst was flushed with H<sub>2</sub> and temperature programmed in H<sub>2</sub>.

The TPD results from catalysts T1, T6 and T13 were reported previously.<sup>1</sup> In this report, data were obtained on catalysts T9, T11 and T15 (pure MnO). Table 1 presents a qualitative listing of the TPD results obtained from the mass spectrometer data for the catalysts studied so far. The composition of the catalysts are also listed. The composition ranged from pure iron (T1) to pure MnO (T15).

In general, CO adsorption occurred to varying degrees with all the catalysts containing iron. During TPD (Step 1) some of the CO desorbed but some remained on the catalyst, most likely as adsorbed surface C and O species. Small amounts of CO<sub>2</sub> produced in the TPD probably arose from reaction between CO and adsorbed O. Subsequent TPR (Step 2) formed CH<sub>4</sub> and H<sub>2</sub>O by reaction of the surface species with H<sub>2</sub>. Similar results were obtained during TPR of adsorbed CO on the catalyst (Step 3) and on the carburized catalyst (Step 4). However, in the latter case, much larger amounts of CH<sub>4</sub> were formed from reaction of the iron carbide phase with H<sub>2</sub>. Pure MnO did not adsorb CO nor did it undergo carburization.

All of the catalysts except T15 (pure MnO) produced methane when exposed to H<sub>2</sub>. The methane formed from residual carbon (Step 2) generally required a higher temperature than that formed with preadsorbed CO (Step 3). A small amount of MnO promoter increased methane evolution but additional amounts of MnO seemed to decrease methane evolution. The presence of varying amounts of MnO had little effect on the temperature of methane production, except for the pure iron catalyst, which formed methane at a lower temperature. After treatment with synthesis gas (at 250°C for 2 hr), the promoted catalysts produced very large methane peaks when temperature programmed in H<sub>2</sub> (Step 4).

The temperature of water evolution in Step 2 seems to increase with increasing MnO content in the catalysts. Manganese oxide is very sensitive to oxygen and could strongly chemisorb oxygen on its surface. The oxygen bonding characteristics of the catalyst will be investigated further. Except for T6, very little water was apparently formed during Step 3. Since no carbon dioxide was detected, it is difficult to explain the methane formation from adsorbed CO without a mechanism for oxygen removal. However, analysis of water evolution characteristics of the catalyst is hampered by possible condensation in the lines leading to the mass spectrometer and occasional apparent presence of oxygen contamination.

The evolution of CO generally occurred at low temperatures (50-100°C) and this weakly adsorbed carbon monoxide was observed on all catalysts but

T15. The latter result agrees with some preliminary adsorption results which showed a lack of adsorption of CO on MnO. In addition, some catalysts showed a very small high temperature evolution of CO. Any strongly adsorbed CO is apparently removed by reaction with H<sub>2</sub> or possibly via disproportionation to CO<sub>2</sub>.

Carbon dioxide evolution was usually small but increased somewhat for catalysts heavily promoted with MnO. Step 1 showed the most consistent CO<sub>2</sub> evolution. In the presence of H<sub>2</sub> (Steps 2, 3, 4), CO<sub>2</sub> evolution was generally eliminated. The carbon dioxide production seen in Step 1 will be investigated further to establish that no possible contaminate oxygen was present. The TPD and TPR experiments, though potentially very revealing, have yielded somewhat inconsistent results so far. Part of the problem is due to the low surface areas of the catalysts under investigation. The mass spectrometer has also been subject to a variety of operational difficulties. However, continued experiments done in close succession will be carried out to establish reproducibility and help clarify trends.

The MnO catalyst was generally inactive with respect to the TPD/TPR experiments. This behavior supports the idea that MnO modifies the iron-based phase of the catalyst but is not active itself in hydrocarbon formation. Whether MnO has an active function in the overall mechanism of the reaction has yet to be established.

#### Future Work

Some of the TPD/TPR experiments will be repeated taking special care that possible oxygen impurity in the helium is eliminated. Studies will begin on H<sub>2</sub>, CO and O<sub>2</sub> chemisorption on the various catalysts to determine metal areas, and BET measurements will be made to compare to metal areas.

#### Reference

1. W.H. Wiser, F.E. Massoth and K.B. Jensen, DOE Contract No. DE-AC01-79ET14700, Quarterly Progress Report, Salt Lake City, Utah, Apr-June 1980.

Table 1. Summary of TPD/TPR results for Fe/Mn Catalysts.

Product	Catalyst <sup>a</sup>	STEP <sup>b</sup>			
		CO/TPD 1	H <sub>2</sub> /TPR 2	CO/TPR 3	Carburized/TPR 4
CH <sub>4</sub>	T1	nil	vs(325-500)	nil	---
	T6	nil	l(400-500)	m(350-500)	vl(400-500)
	T9	nil	s(400-450)	vs(280-330)	vl(375-500)
	T11	nil	m(400-490)	s(250-500)	vl(340-500)
	T13	nil	s(400-500)	s(350-500)	vl(400-500)
	T15	nil	nil	nil	nil
H <sub>2</sub> O	T1	nil	m(270-370)	nil	---
	T6	nil	m(250-500)	vl(250-500)	m(300-450)
	T9	nil	m(410-500)	vs(400-500)	s(450-500)
	T11	nil	s(450-500)	nil	vs(350-450)
	T13	nil	{ vs(200-250) s(450-500)	vs(475-500)	m(300-450)
	T15	nil	s(450-500)	nil	nil
CO	T1	vs(50-100)	nil	nil	---
	T6	s(50-100)	nil	{ m(50-150) s(350-450)	vs(400-500)
	T9	{ s(70-120) s(420-500)	nil	vs(70-120)	vs(25-150)
	T11	{ s(70-150) vs(470-500)	nil	s(75-150)	vs(70-120)
	T13	vs(50-100)	s(300-450)	{ m(80-150) s(400-500)	{ s(80-150) s(350-450)
	T15	nil	nil	nil	nil
CO <sub>2</sub>	T1	nil	nil	nil	---
	T6	vs(80-350)	nil	nil	nil
	T9	vs(170-350)	nil	nil	nil
	T11	vs(170-350)	vs(25-200)	nil	nil
	T13	s(150-350)	s(50-200)	nil	vs(350-425)
	T15	nil	vs(180-220)	nil	nil

<sup>a</sup>Compositions: T1-Fe, T6-0.06 Mn/Fe, T9-0.18 Mn/Fe, T11-0.63 Mn/Fe, T13-2.78 Mn/Fe, T15-MnO.

<sup>b</sup>Values in ( ) are temp ranges in °C. Relative peak heights: vs-very small, s-small, m-moderate, l-large, vl-very large.

## V. Conclusions

Detailed conclusions are included in the reports for each task. Task 1 is temporarily inactive, awaiting a student. Tasks 9 and 11 have not been initiated as yet. No work was done under Task 15.